# Development of immunohistochemistry based molecular classification of colorectal carcinomas: a correlation between transcriptome analysis and immunohistochemical study

Jang, Mi

Department of Medicine

The Graduate School, Yonsei University

# Development of immunohistochemistry based molecular classification of colorectal carcinomas: a correlation between transcriptome analysis and immunohistochemical study

Jang, Mi

Department of Medicine

The Graduate School, Yonsei University

# Development of immunohistochemistry based molecular Classification of colorectal carcinomas: a correlation between transcriptome analysis and immunohistochemical study

Directed by Professor Kim, Hoguen

The Doctoral Dissertation
submitted to the Department of Medicine,
the Graduate School of Yonsei University
in partial fulfillment of the requirements for the degree
of Doctor of Philosophy

Jang, Mi

June 2019

This certifies that the Doctoral Dissertation of Jang, Mi is approved.

---

Thesis Supervisor: Kim, Hoguen

---

Thesis Committee Member#1: Kim, Tae Il

---

Thesis Committee Member#2: Min, Byeong So

---

Thesis Committee Member#3: Kim, Han Kyeom

---

Thesis Committee Member#4: Paik, Soonmyung

The Graduate School
Yonsei University

June 2019

# ACKNOWLEDGEMENTS

First and foremost, I would like to praise and thank the Lord, God Almighty. I thank God for enlightening my life with Divine Providence. He provided the strength to undertake the research as a medical doctor. I learned how to trust in Him and realized how much I'm being loved by family and faithful friends.

With great appreciation, I want to thank my advisor, Professor. Hoguen Kim. It has been an honor to be his last Ph.D. student. His scholarly advice, scientific approach, and funding have been instrumental in helping me accomplish the study. I also express sincere gratitude to Prof. Soonmyung Paik, Prof. Han Kyeom Kim, Prof. Tae Il Kim, and Prof. Byeong So Min. The guidance, suggestions, and constructive criticism have greatly helped my scientific development and research. I'm deeply grateful to Prof. Won Kyu Kim, Prof. Xianglan Zhang, Prof. Ki-Youl Kim, Yujin Kwon, Minhee Park for their scientific help, support throughout this study, and all words of encouragement. I would like to thank all professors and colleagues (especially Dr. Hyang Sook Jeong and Dr. Hayoung Woo, who completed the medical residency program together) in the Department of Pathology, Yonsei University College of Medicine and Severance Hospital. My very special thanks go to my dearest friends, Eun Kyung Kim, Hyo Jeong Oh, Hyunjin Park, Jeong Sim Kim, and Seoyon Park (alphabetically arranged) for their love and encouragement. I'm grateful for the memories we share since medical school and you all are very special in my life. I also want to extend my appreciation to Dr. Seong Min Han for unconditional affection.

I dedicate this Ph.D. thesis to my family, my mom, dad, my sisters So Ra and Young In, my brother-in-laws Jeongyeol, my sweetheart nephew Ye Joon, and grandmother, for love throughout my life and during this study. Mom and dad, I do not know how to thank you enough for your support to be who I am today. I love you all so much.

# <TABLE OF CONTENTS>

ABSTRACT ····· 1
I. INTRODUCTION ····· 3
II. MATERIALS AND METHODS ····· 5
1. Clinical Samples ····· 5
2. RNA preparation ····· 6
3. Gene expression analysis ····· 6
4. mRNA gene expression data preparation and statistical analysis ····· 7
5. Molecular subtyping and comparison to the published consensus molecular subtype ····· 8
6. Microsatellite instability assay ····· 9
7. KRAS and BRAF mutation analysis ····· 9
8. Tissue microarray construction ····· 9
9. Immunohistochemistry for IHC classifier ····· 10
10. Immunoscore assessed by using median cut-offs ····· 15
11. Histologic parameter interpretation ····· 16
12. The IHC classifier construction ····· 17
13. Statistical analysis ····· 18
14. Ethical compliance ····· 19
III. RESULTS ····· 19
1. The clinicopathologic features of the CRC patients ····· 19
2. Unsupervised clustering analysis of mRNA expression profiles identifies four distinct molecular subtypes ····· 21
3. Gene expression-based molecular subtypes are categorized in four groups by nonnegative matrix factorization ····· 23
4. Correlation between NNF based and CMS ····· 25
5. Clinicopathologic characteristics of CRCs according to the molecular subtypes ····· 26

6. Identification of subtype specific markers ····· 33
7. Establishment of the IHC subtype classifier to predict molecular subtype ····· 35
8. Similarities of the clinicopathologic characteristics of the predicted subtypes by IHC classifier and the molecular subtypes by transcriptome 37
9. Correlation between NMF-based groups and CMSs subtyped by IHC classifier ····· 42
10. Patients survival analysis ····· 44
11. Differentially predicted subtype at the tumor center and invasion margin ····· 54
IV. DISCUSSION ····· 58
V. CONCLUSION ····· 63
REFERENCES ····· 64
ABSTRACT (IN KOREAN) ····· 71
PUBLICATION LIST ····· 73

# LIST OF FIGURES

Figure 1. Immunoprofiles of the selected markers ····· 15
Figure 2. Study design ····· 21
Figure 3. Unsupervised hierarchical clustering analysis of mRNA expression profiles from colon cancer tissue ····· 22
Figure 4. Four molecular subtypes identified using consensus clustering based NMF ····· 24
Figure 5. Histologic features according to the molecular subtypes ····· 32
Figure 6. Identification of mRNAs differentially expressed in each of the four groups, as compared to non-neoplastic colon mucosa tissue and/or the other groups ····· 34
Figure 7. Accuracy and AIC of the IHC classifiers ····· 37
Figure 8. Histologic features according to the predicted subtypes ····· 42
Figure 9. Comparison of survival analysis of molecular subtypes classified by transcriptome analysis and IHC classifier in cohort 1 ····· 46
Figure 10. Survival analysis of the predicted subtypes of validation cohort ····· 47
Figure 11. Survival analysis of the predicted CMS of stage III CRCs with FOLFOX adjuvant therapy ····· 58
Figure 12. Differentially predicted subtypes at the tumor center and invasion margin ····· 54
Figure 13. The immumoprofiles of the case 1-43 ····· 57

# LIST OF TABLES

Table 1. Information of the selected IHC markers based on molecular classification ····· 12
Table 2. Criteria of the immunoscore calculation ····· 16
Table 3. Clinicopathologic features of the CRC patients of cohort 1 and cohort 2 ····· 20
Table 4. Correlation between NMF-based groups and CMS subtypes ···· 26
Table 5. Clinicopathologic features of cohort 1 according to the CMS subtype ····· 28
Table 6. Clinicopathologic features of cohort 1 according to the NMF molecular subtype ····· 30
Table 7. The IHC classifier to predict subtypes····· 36
Table 8. Clinicopathologic characteristics of the predicted CMS according to the IHC classifier····· 39
Table 9. Correlation between NMF based groups and CMS subtypes of cohort 2 ····· 43
Table 10. Univariate and multivariate Cox-proportional hazards models for OS····· 50
Table 11. Univariate and multivariate Cox-proportional hazards models for DFS····· 52
Table 12. Differentially predicted CMS at the tumor center, invasion margin, and metastatic lesion····· 56

ABSTRACT

**Development of immunohistochemistry based molecular classification of colorectal carcinomas: a correlation between transcriptome analysis and immunohistochemical study**

Jang, Mi

*Department of Medicine,*
*The Graduate School, Yonsei University*

(Directed by Professor Kim, Hoguen)

The current standard treatment of stage III colorectal cancers involves adjuvant chemotherapy with FOLFOX after curative resection; however, the clinical outcomes of this therapy are variable. For personalized therapeutic strategy after curative resection, identification of eligible biomarkers and subsequent molecular classification to predict the outcomes of the FOLFOX regimen is warrented. In this study, I aimed to investigate the practical molecular subtype by analyzing the mRNA expression profile of stage III CRC followed by FOLFOX, searching subtype classifying genes, and establishing algorithms for the immunohistochemical assessment of each subtype.

I developed non-negative matrix factorization (NMF) based four molecular subtypes using a training cohort (n = 101, stage III CRCs with FOLFOX treatment). I found that these four subtypes have many similarities to the consensus molecular subtypes (CMS) of CRCs. I selected thirteen markers available for IHC that overexpressed by >1.5 fold relative in one group to that of the other three groups and normal mucosa and included other 19 previously proposed immunohistochemical, molecular markers for the classification of molecular subtypes. I finally selected nine

IHC factors that showed a significant difference in expression between groups. To predict CMS, I selected SNAI1, MUC2, SPINK4, KIT, CDX2, ZMYND8, TFF3, MUC5AC, and MSI status using MMR markers (accuracy: 0.825, 95% CI = 0.737 - 0.825, AIC: 134.771, 95% CI = 134.507 - 160.549). As expected, application of the validation cohort (n = 401) revealed subtype-specific characteristics and poor prognosis of CMS4. Using the IHC classifier, I found that CMS3 and CMS4 are the groups that have a bad prognosis in FOLFOX chemotherapy. My study proposes the practical IHC classifier predicting a prognosis of CRCs after standard therapy in stage III CRCs.

Key words: colorectal cancer, mRNA expression-based molecular classification, molecular subtype, consensus molecular subtype, immunohistochemical stain based subtype classifier, FOLFOX chemotherapy,

Abbreviations: CRC; colorectal carcinoma, MSI; microsatellite instability, IHC; immunohistochemicstry, CMS; consensus molecular subtypes, NMF; non-negative matrix factorization, TSP; tumor stromal percentage, KM grade; Klintrup–M€akinen grade, GMS; Glasgow microenvironment score, AIC: Akaike's information criterion

# Development of immunohistochemistry based molecular classification of colorectal carcinomas; a correlation between transcriptome analysis and immunohistochemical study

Jang, Mi

*Department of Medicine,*
*The Graduate School, Yonsei University*

(Directed by Professor Kim, Hoguen)

## I. INTRODUCTION

Colorectal cancer (CRC) is the third most common cancer worldwide, with a 5-year overall survival of 65% [1,2]. At present, the prognosis is based predominantly on the pathological stage of the disease. There is an urgent need to establish a classification strategy to identify the patient group that may benefit from adjuvant therapy.

For stage III CRCs, standard therapy includes curative surgery, followed by adjuvant chemotherapy with the FOLFOX (oxaliplatin plus infusional 5-fluorouracil [5-FU] and leucovorin) regimen based on the MOSAIC trial [3,4]. Adjuvant chemotherapy is associated with an approximately 30% reduction in the risk of disease recurrence, and a 22% to 32% reduction in mortality. Oxaliplatin is a typical cause of the debilitating side effects associated with long-term sensory neuropathy and impairment of quality of life [5]. Individual patients react to the drugs differently, and these diverse responses to the adjuvant chemotherapy reveal tumor heterogeneity.

Currently, there are known molecular characteristics that provide limited predictive value for drug response. For instance, studies have suggested that tumors with high-level microsatellite instability (MSI-High) may be less

responsive to 5-fluorouracil[6,7]. Detection of mutations in the KRAS/BRAF axis is crucial for predicting resistance to epidermal growth factor receptor (EGFR)-targeted therapy in metastatic diseases [8,9]. However, currently available molecular markers provide only limited information, particularly in chromosomal instability where the large heterogeneous drug responses are unexplained.

Several studies on molecular heterogeneity in CRCs have used gene expression-based data to assess disease stratification [10-17]. Recently, an international consortium analyzed the interrelation of the previously published CRC subtypes and proposed four consensus molecular subtypes (CMSs) [11-15,17,18]. These include a microsatellite-instability, mucinous, inflammatory subtype (CMS1, 14%); an epithelial subtype with marked WNT and MYC signaling activation (CMS2, 37%); an epithelial subtype with metabolic dysregulation (CMS3, 13%); and a mesenchymal-like subtype exhibiting epithelial mesenchymal transition (EMT), microsatellite stability, angiogenesis, and hyperactivation of transforming growth factors(TGF-β) (CMS4, 23%). Unclassified phenotypes (13%) showed mixed features. CMS 4 is well known as a poor prognostic and shows similar poor prognosis in response to chemotherapeutic agents including oxaliplatin[18,19].

Even though these molecular subtypes can predict clinicopathologic characteristics and the natural prognosis of the disease, still more information is needed to estimate the prognoses of stage III CRCs after administration of the FOLFOX chemotherapeutic regimen.

Specifically, evaluating the response to FOLFOX adjuvant chemotherapy according to molecular subtypes may provide insights into 1) the natural course of stage III CRCs after FOLFOX chemotherapy according to molecular subtype and 2) the identification of specific subgroup(s) that derive the greatest benefit from FOLFOX chemotherapy.

In the present study, I established two cohorts: the training cohort (cohort 1), comprising stage III CRCs treated with FOLFOX adjuvant chemotherapy and the validation cohort (cohort 2), comprising stage I-IV CRCs. I selectively used fresh frozen tissues samples from the training cohort. Homogeneous tumor cell populations (> 70% tumor cells) of each tissue were collected using

microdissection, which allowed us to minimize experimental error caused by the presence of a differential proportion of tumor cells in tissue samples. I analyzed mRNA expression profiles of stage III CRC samples and matched non-neoplastic colon mucosal tissues. In doing so, I identified colon cancer-specific transcripts and further found that CRC gene expression profiles can be divided into four types by nonnegative matrix factorization (NMF). I demonstrated an association between our specific molecular subtypes and the CMS, and further identified prognosis of each subtype treated with FOLFOX chemotherapy in stage III CRCs. I selected subtype-specific markers based on the gene expression profiles and established immunohistochemistry (IHC) classifiers to predict NMF-based group and CMS.

## II. MATERIALS AND METHODS

### 1. Clinical Samples

The study cohort was a retrospective cohort retrieved from the pathology archive. Patient cohort 1, training cohort, consisted of 101 CRCs which were stage III (metastasis to regional lymph nodes but not distant sites) treated with the FOLFOX regimen as adjuvant chemotherapy. The cohort 2, validation cohort, consisted of 401 CRCs from stage I to stage IV.

The selected cases were reviewed according to WHO 4th edition 2010 criteria and staged according to the 7th edition of the American Joint Committee on Cancer TNM classification system. Demographic data and clinicopathologic characteristics were obtained from medical records.

Formalin-fixed paraffin-embedded (FFPE) tumor tissues and fresh frozen tissues of cohort 1 were obtained from the patients with colorectal adenocarcinoma who underwent surgical resection from January 2006 to December 2012 at Severance Hospital, Korea. Formalin-fixed paraffin-embedded (FFPE) tumor tissues of cohort 2 were obtained from the patients with colorectal adenocarcinoma who underwent surgical resection from January 2010 to December 2012 at Severance Hospital, Korea. The tissue specimens were obtained from the archives of the

Department of Pathology, Yonsei University, Seoul, Korea and from the Liver Cancer Specimen Bank of the National Research Resource Bank Program of the Korean Science and Engineering Foundation of the Ministry of Science and Technology.

**2. RNA preparation**

A total of 101 CRCs and 35 matched non-neoplastic colon mucosal fresh frozen tissue samples of the cohort 1 underwent microdissection using a cryostat and was fractionated to improve the tumor content. Prior to cutting sections for RNA isolation, a slide was reviewed by hematoxylin-eosin staining to allow the selection of samples with >70% tumor cells; samples with a tumor cell content <70% were further cut to enrich the tumor cell population. Through this process, I ensured that all samples analyzed in this study comprised of >70% tumor cells. Total RNA was extracted using TRIzol Reagent (Invitrogen Life Technologies, Carlsbad, CA, USA), according to the manufacturer's protocol. After DNase digestion and other clean-up procedures, RNA samples were quantified, aliquoted, and stored at -80°C until use. For quality control, RNA purity and integrity were evaluated by denaturing gel electrophoresis and by measuring the A260/280 ratio. All samples were analyzed using the 2100 Bioanalyzer (Agilent Technologies, Santa Clara, CA, USA). For all samples, the RNA integrity number scores were >9.5.

**3. Gene expression analysis**

For DNA microarray hybridization, RNA was pooled by mixing equal amounts of total RNA, and biotin-labeled cRNA targets were synthesized starting from 1.5 μg of total RNA. Double-stranded cDNA synthesis was performed using the Illumina® TotalPrep RNA Amplification Kit (Illumina, San Diego, CA, USA), while biotin-UTP-labeled antisense RNA was transcribed in vitro using the Ambion MEGAscript kit (Ambion Life Technologies, Carlsbad, CA, USA). All steps of the labeling procedure were performed according to the manufacturers' protocols. Microarray experiments were conducted on the HumanHT-12 v4

Sentrix Expression BeadChip (Illumina), which contains 47,231 probes, representing 31,332 annotated genes. Hybridization of labeled cRNA to the BeadChip, washing, and scanning were performed according to the Illumina Bead Station 500× manual.

**4. mRNA gene expression data preparation and statistical analysis**

Raw data were extracted using the software provided by the manufacturer (Illumina Genome Studio v2011.1 [Gene Expression Module v1.9.0]), and expression intensities were normalized using quantile normalization techniques [20]. Based on these normalized intensities, genes differentially expressed in non-neoplastic colon mucosal tissues and colon tumors were determined using the integrated statistical method as previously reported [21]. Briefly, two independent tests were performed: a Student's t-test and the log2-median-ratio test. Adjusted P-values from each test were computed using an empirical distribution of the null hypothesis that the means of the genes are not different, which was obtained from random-permutations of the samples. The P-values from the two tests were combined to compute the overall P-values using Stouffer's method[22], and for unsupervised hierarchical clustering, 4,823 DEGs were selected from the microarray raw data under the conditions of |fold change|>2 and P-value<0.05. For NMF consensus clustering analysis, 1,764 DEGs were selected from the microarray raw data under the conditions of |fold change|>2 and P-value<0.01, and 1,538 DEGs were selected from DEGs among tumor groups that were divided by unsupervised hierarchical clustering under the conditions of |fold change|>2 and P-value<0.01. For gene expression analysis |fold change|>1.5 and P-value<0.01 were applied to obtain DEGs belonging to CRCassigner-30, which was a group of 30 genes with high scores calculated by PAM (nearest shrunken centroids–based method) [23] reported in a previous study [17]. Finally, functional enrichment analysis of the differentially expressed genes was performed using DAVID software [24] in order to identify GO biological processes and Kyoto Encyclopedia of Genes and Genomes (KEGG) pathways represented by the genes in individual clusters with statistical significance.

**5. Molecular subtyping and comparison to the published consensus molecular subtype**

For molecular subtyping, I applied a hierarchical clustering and nonnegative matrix factorization (NMF)[25-27], using the gene expression profiles from CRC tissues. In brief, NMF consensus clustering method resorts to factor the gene-expression matrix A into the product of two matrices of positive entries, A ~ WH. Matrix W has size N × k and Matrix H has size k × M. k is much smaller than M. The column of W defines a 'metagene', with entry wij the coefficient of the gene I in metagene j. The columns of Matrix H represent the metagene expression pattern of the corresponding sample, with each entry hij representing the expression level of metagene i in sample j. Given factorization of A ~ WH, Matrix H can be used to determine the cluster membership: sample j is placed in cluster i if the hij is the largest entry in column j[25]. Differentially expressed genes were selected using complete linkage for hierarchical clustering based on the Pearson coefficient correlation algorithm, and these were utilized for NMF with MATLAB software. Molecular subtyping was performed with consensus clustering-based NMF, according to the optimal number of clusters, which was determined based on the cophenetic correlation coefficient (coph) values [27,28] determined in our previous study (coph=0.8961). I performed a repeated NMF clustering analysis using the same set of samples with 1,764 DEGs under the same condition, and confirmed that the four groups divided by type 1 clustering were reproducible (93% matched). To subtype our samples by another method, I adopted Ward's minimum variance method in combination with Euclidean distance and weighted gene co-expression network analysis (WGCNA) [29]. WGCNA was used to verify the quality of our microarray data, and Ward's minimum variance method according to Euclidean distance was used to cluster 101 colorectal tumors. To compare our molecular subtypes with the previously reported CMSs, I used CMSclassifier [18], which includes the random forest classifier, as well as a 'single-sample predictor' (SSP) classifier. Further, the prognosis predicting values of our molecular subtypes and CMS subtypes were compared and analyzed by 'CMS classifier'.

**6. Microsatellite instability assay**

For microsatellite instability analysis, I carried out both molecular test and the immunohistochemical stain test. (Table 1) For molecular analysis, the NCI panel, composed of BAT26, BAT25, D5S346, D2S123, and D17S250 markers, was tested. PCR products were analyzed by capillary electrophoresis. For interpretation, instability at more than one locus was defined as MSI-H, instability at a single locus was defined as low MSI (MSI-L), and no instability at any locus was defined as MSS. For the immunohistochemical stain test, MLH1, MSH2, MSH6, and PMS2 antibodies were used. Loss of expression in at least one protein was interpreted as MSI-High.

**7. KRAS and BRAF mutation analysis**

KRAS mutation analysis was performed to cohort 1 via pyrosequencing, using the CE-IVD Marked PyroMark KRAS Kit (QIAGEN, Hilden, Germany), according to the manufacturer's protocols (Therascreen KRAS Pyro Kit Handbook, version 1, July 2011). For each sample, 10 ng of genomic DNA was used for the analysis of mutations in codons 12 and 13 and another 10 ng DNA was utilized to identify mutations in codon 61. Pyrosequencing was also employed for BRAF mutation analysis to detect the BRAF V600E mutation, as previously reported [30].

**8. Tissue microarray construction**

On H&E stained slides of tumors, the representative area was selected and the corresponding spot was marked on the surface of the paraffin block. Using a manual tissue microarrayer, the selected area was punched out and a 3-mm tissue core was placed into a 6 × 5 recipient block. Two tissue cores of tumor center and one tissue core of periphery of the tumor showing invasion margin were extracted. The tissue core from the metastatic lymph node of 100 cases was extracted too. Each tissue core was assigned a unique tissue microarray (TMA) location number that was linked to a database containing its clinicopathologic data.

**9. Immunohistochemistry for IHC classifier**

Paraffin-embedded tissue blocks were cut into 4-mm sections. Immunohistochemical analysis was performed using a Ventana XT automated stainer (Ventana, Tucson, AZ, USA). I performed the immunohistochemical stain to the CRCs using the following antibodies (Table 1).

Among the markers showing significantly different mRNA expression between molecular subtypes, 13 markers available for IHC were included as candidate markers for IHC classifier. An additional 19 markers previously suggested as CMS classifying markers showing different gene expression between molecular subtypes were included. MLH1, MSH2, MSH6, and PMS2 were used to evaluate the MSI status. A total 32 genes were selected and IHC were performed. Among them 19 markers were excluded due to stain failure and insignificant IHC expression between subtypes. Finally I selected SPINK4, MUC2, MUC5AC, TFF3, CDX2, HTR2B, KIT, SNAI1, ZMYND8, and MSI status to establish the IHC subtype classifiers (Figure 1).

The H-score method, which is a widely used IHC interpretation method, was adopted. This method assigns an IHC H-score to each case on a continuous scale of 0–300, based on the percentage of cells at different staining intensities. Nuclear or cytoplasmic staining was scored within four categories: 0 for ‘no staining’, 1 + for ‘weak staining visible at high magnification’, 2 + for ‘intermediate staining’ and 3 + for ‘strong staining’. The percentage of cells at different staining intensities was determined by visual assessment, with the score calculated using the formula 1 × (% of 1 + cells) + 2 × (% of 2 + cells) + 3 × (% of 3 + cells). The stain interpretation was then classified as either low or high protein expression according to the antibody specific cut-off value. The cut off value of the antibody; SPINK4: 20, MUC2: 10, MUC5AC: 10, FAM81A: 100, TFF3: 10, HTR2B: 100, SNAIL: 20, CDX2: 150, ACSL6: 100, PDGFRB: 100, HOPX: 200, and ZEB1: 70. An H-score value higher than the cut off value was considered as high expression, and value lower than the cut off value was considered as low expression. For ZMYND8, if the staining intensity was weaker than normal mucosa, it was considered as lower expression, and otherwise considered as high expression. For KIT, DEFA5, DSC3, TAGLN, NOX4, TSPAN6, PDGFRA, and PDGFC, any

proportion of protein expression was classified into positive, otherwise negative. For ZMYND8, if the intensity was weaker than normal gland, it was considered as low expression, and an intensity same as or stronger than normal gland, it was considered as high expression. For CTNNB1 (beta-catenin), nuclear expression of more than 10% was counted as positive, otherwise negative.

**Table 1. Information of the selected IHC markers based on molecular classification**

| Target CMS | Target NMF group | Markers | Inclusion | | Exclusion | Selected as final IHC marker |
|---|---|---|---|---|---|---|
| | | | group specific mRNA expression | suggested in previous study | | |
| 3[12] | 1 | SPINK4 | ○* | ○ | | ○ |
| 3[17,31-33] | 1 | MUC2 | ○ | ○ | | ○ |
| 3 | 1 | DEFA5 | ◎** | | insignificant IHC expression | |
| 1,3 | 1,2 | MUC5AC | ◎ | | | ○ |
| 1 | 2 | FAM81A | ◎ | | insignificant IHC expression | |
| 1[17,31] | 2 | TFF3 | ○ | ○ | | ○ |
| 1,4[13,31,32] | 2,3 | CDX2 | ○ | ○ | | ○ |
| 1[17,18] | 2 | MLH1 | | ○ | | ○ |
| 1[17,18] | 2 | MSH2 | | ○ | | ○ |
| 1[17,18] | 2 | MSH6 | | ○ | | ○ |
| 1[17,18] | 2 | PMS2 | | ○ | | ○ |
| 1 | 2 | MOCOS | ◎ | | IHC stain fail | |
| 4 | 3 | HOPX | ◎ | | insignificant IHC expression | |
| 4[13,32] | 3 | HTR2B | ○ | ○ | | ○ |
| 4 | 3 | MYL9 | ◎ | | insignificant IHC expression | |
| 4 | 3 | TAGLN | ◎ | | insignificant IHC expression | |

| | | | | | | |
|---|---|---|---|---|---|---|
| 4[17,32] | 3 | ZEB1 | | ○ | insignificant IHC expression | |
| 4[17] | 3 | SNAI1 | ○ | ○ | | ○ |
| 4[34] | 3 | NOX4 | ○ | ○ | insignificant IHC expression | |
| 4[35] | 3 | PDGFRA | ○ | ○ | insignificant IHC expression | |
| 4[35] | 3 | PDGFRB | ○ | ○ | insignificant IHC expression | |
| 4[35] | 3 | PDGFC | ○ | ○ | insignificant IHC expression | |
| 4[35] | 3 | KIT | ○ | ○ | | ○ |
| 4[32] | 3 | KRT | | ○ | insignificant IHC expression | |
| 4 | 3 | PRRX1 | ◎ | | Failure of IHC stain | |
| 4 | 3 | SPARC | ◎ | | Failure of IHC stain | |
| 4 | 3 | FRMD6 | ○ | ○ | Failure of IHC stain | |
| 2 | 4 | DSC3 | ◎ | | insignificant IHC expression | |
| 2 | 4 | ZMYND8 | ◎ | | | ○ |
| 2 | 4 | ACSL6 | ◎ | | insignificant IHC expression | |
| 2 | 4 | TSPAN6 | ◎ | | insignificant IHC expression | |
| 2[17,18] | 4 | CTNNB1 | | ○ | insignificant IHC expression | |

*○: group specific expression with >1.0 fold, **◎: group specific expression with >1.5 fold and p-value <0.05, MLH1, MSH2, MSH6, and PMS2 was analyzed for MSI status, Primary antibody information: SPINK4(HPA007286, Sigma-

Aldrich, St. Louis, MO, USA, 1/100), MUC2(MRQ-18, Cell marque Rocklin, CA, USA, 1/100), DEFA5(HPA015775, Sigma-Aldrich, St. Louis, MO, USA, 1/400), MUC5AC(MRQ-19, Cell marque Rocklin, CA, USA, 1/100), TFF3(15C6, Merck Millipore, Darmstadt, Germany, 1/100), FAM81A(HPA001847, Sigma-Aldrich, St. Louis, MO, USA, 1/100), MLH1(554073, BD Biosciences, San Jose, CA, USA, 1/50), MSH2(556349, BD Biosciences, San Jose, CA, USA, 1/200), MSH6(44, Cell Marque Rocklin, CA, USA, 1/100), PMS2(MRQ-28, Cell Marque Rocklin, CA, USA, 1/40), HOPX(SC-30216,Santa Cruz, Dallas, TX, USA,1/100), HTR2B(HPA012867, Sigma-Aldrich, St. Louis, MO, USA, 1/400), TAGLN(HPA019467, Sigma-Aldrich, St. Louis, MO, USA, 1/25), ZEB1(HPA027524,Sigma-Aldrich, St. Louis, MO, USA,1/500), SNAIL(LS-C176686-100, LifeSpan Biosciences, Seattle, WA, USA, 1/100), NOX4(ab133303, Abcam, Cambridge, United Kingdom, 1/100), PDGFRA(ab65258, Abcam, Cambridge, United Kingdom, 1/100), PDGFRB(ab69506, Abcam, Cambridge, United Kingdom, 1/400), PDGFC(ab200401, Abcam, Cambridge, United Kingdom, 1/200), CKIT(ab5505,Abcam, Cambridge, United Kingdom,1/400), KRT[CK(AE1/AE3), M3515, Dako, Glostrup, Denmark, 1/600], CDX2(EPR2764Y,Cell Marque Rocklin, CA, USA, 1/400), DSC3(61093, PROGEN Biotechnik, Heidelberg, Germany, 1/50), ZMYND8(HPA020949, Sigma-Aldrich, St. Louis, MO, USA, 1/800), ACSL6(HPA040470, Sigma-Aldrich, St. Louis, MO, USA, 1/50), TSPAN6(HPA004109, Sigma-Aldrich, St. Louis, MO, USA,1/100), CTNNB1(610153, BD Biosciences, San Jose, CA, USA, 1/200), CD3(IS503 LOT 20017497, Dako, Glostrup, Denmark, prediluted), CD8(C8/144B, Dako, Glostrup, Denmark, prediluted), PRRX1 (NBP2-13816; Novus Biologicals, Centennial, CO, USA), LUM(HPA001522, Sigma-Aldrich, St. Louis, MO, USA), MOCOS (ab150852, Abcam, Cambridge, United Kingdom), RPL8(HPA045095, Sigma-Aldrich, St. Louis, MO, USA), SPARC(33-5500, Invitrogen, Carlsbad, CA, USA), VCAN(MABT16, Merck Millipore, Darmstadt, Germany), FRMD6(CSB-PA822270ESR2HU, cusabio, Houston, TX, USA)

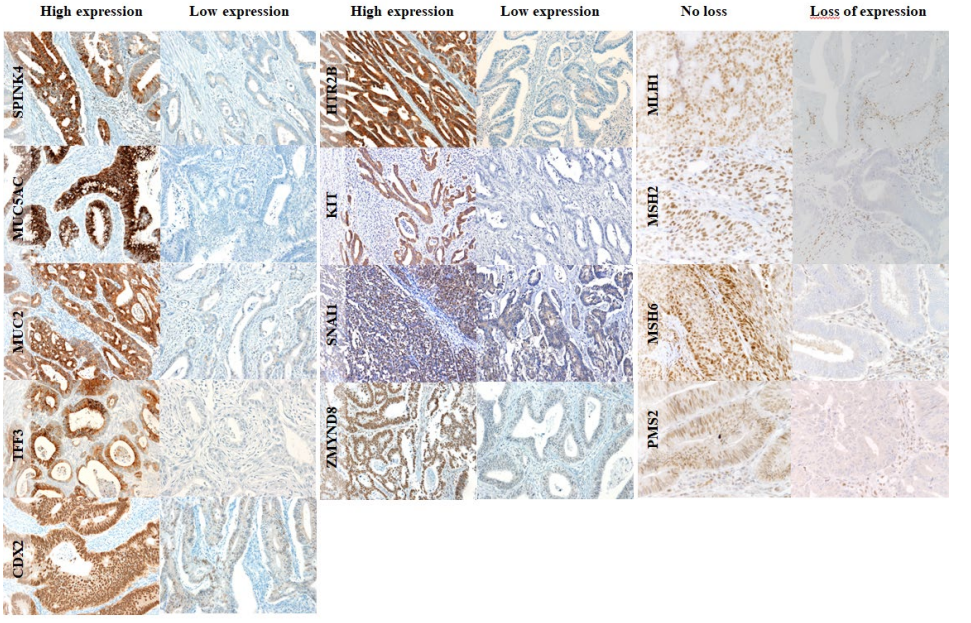


**Figure 1. Immunoprofiles of the selected markers.** High expression and low expression was counted using marker specific H-score cut off values.

**10. Immunoscore assessed by using median cut-offs**

To measure CD3 positive or CD8 positive T lymphocyte density, all stained TMA slides were scanned (magnification ×200) with a VENTANA iScan HT slide scanner (Ventana Medical Systems). The digital slides were analyzed by VENTANA Virtuoso Digital Pathology Image Analysis software Version 5.3 (Ventana Medical Systems, Inc, Sunnyvale, CA) and explored to evaluate areas of insufficient quality such as scanning errors. Cell Counter plug-in of ImageJ platform (http://rsb.info.nih.gov/ij/index.html) was employed to quantify the number of positively stained cells in cells/mm2 by counting randomly selected three spots in x200 power fields. CD3 or CD8 positive lymphocytes in the center of the tumor and the invasion margin ware counted separately, with the exception of tumor areas with crush artifacts or necrosis. The CD3+ T cell count at the tumor center (CD3 TC), CD3+ T cell count at the invasion margin (CD3 IM), CD8+ T cell count at the tumor center (CD8 TC), and CD8+ T cell count at the invasion

margin (CD8 IM) was translated into high or low according to the mean value of total cohort cases. Then the mean percentile of the four immune parameters is calculated into low, intermediate, and high. (Table2) [36,37]

**Table 2. Criteria of the immunoscore calculation**

| CD3 TC | CD3 IM | CD8 TC | CD8 IM | Mean of 4 markers |
|---|---|---|---|---|
| High | High | High | High | High immunoscore |
| High | High | High | Low | |
| High | High | Low | High | |
| High | Low | High | High | |
| Low | High | High | High | |
| High | High | Low | Low | Intermediate immunoscore |
| High | Low | High | Low | |
| High | Low | Low | High | |
| Low | High | High | Low | |
| Low | High | Low | High | |
| Low | Low | High | High | |
| High | Low | Low | Low | Low immunoscore |
| Low | High | Low | Low | |
| Low | Low | High | Low | |
| Low | Low | Low | High | |
| Low | Low | Low | Low | |

TC: Tumor center, IM: Invasion margin

### 11. Histologic parameter interpretation

가. Tumor stromal percentage (TSP)

The assessment of TSP was carried out using H&E-stained sections of the deepest point of tumor invasion as previously described [38]. The most invasive tumor area on each slide was selected using a ×4 objective. A part of the sample was selected where both tumor and stromal tissue were available using a ×10 objective. Tumor cells must be present at all borders of the image field (north–east–south–west). Areas of necrosis or mucin were excluded from the field. A stromal percentage over the tumor percentage (TSP≥50%), was considered as high TSP, otherwise low TSP.

나. Klintrup–M€akinen (KM) grade

The generalized inflammatory cell infiltrate was assessed using the KM grade as previously described[39]. Briefly, the inflammatory cell infiltrates at the invasive margin was assessed in a semi-quantitative fashion using a 4-point scale (0: no increase, 1: mild or patchy increase in inflammatory cells, 2: prominent inflammatory reaction forming a band at the invasive margin, and 3: florid cup-like infiltrate at the invasive edge with destruction of cancer cell islands) at the haematoxylin and eosin-stained (H&E) slide. For statistical analysis, patients were subsequently classified as low grade (0/1) or high grade (2/3).

다. The Glasgow Microenvironment Score (GMS)

The assessment of GMS was evaluated by the combination of TSP and KM grade as previously described [40]. The detailed scoring system is as follows. GMS 0: a strong KM grade and either high or low TSP, GMS 1: a weak KM grade and low TSP, and GMS 2: a weak KM grade and high TSP.

**12. The IHC classifier construction**

The multinomial logistic model was adopted as a statistical method for four possible outcomes, by running three independent binary logistic regression models. CMS1 or NMF1 was chosen as a "reference" and the outcomes are separately regressed against the reference outcome.

$$\ln(\frac{P(CMS2)}{P(CMS1)}) = \beta_{20} + \beta_{21}(TFF3) + \beta_{22}(SPINK4) + \beta_{23}(KIT) + \beta_{24}(CDX2)$$
$$+\beta_{25}(ZMYND8) + \beta_{26}(MUC2) + \beta_{27}(MUC5AC) + \beta_{28}(MSIstatus) + \beta_{29}(Snail\_nuclear)$$

$$\ln(\frac{P(CMS3)}{P(CMS1)}) = \beta_{30} + \beta_{31}(TFF3) + \beta_{32}(SPINK4) + \beta_{33}(KIT) + \beta_{34}(CDX2)$$
$$+\beta_{35}(ZMYND8) + \beta_{36}(MUC2) + \beta_{37}(MUC5AC) + \beta_{38}(MSIstatus) + \beta_{39}(Snail\_nuclear)$$

$$\ln(\frac{P(CMS4)}{P(CMS1)}) = \beta_{40} + \beta_{41}(TFF3) + \beta_{42}(SPINK4) + \beta_{43}(KIT) + \beta_{44}(CDX2)$$
$$+\beta_{45}(ZMYND8) + \beta_{46}(MUC2) + \beta_{47}(MUC5AC) + \beta_{48}(MSIstatus) + \beta_{49}(Snail\_nuclear)$$

For CMS classification, CMS 1 was chosen as reference, and the three formulas were constructed.

$\ln [P(CMS2)/P(CMS1)]$ =286.6+(-92.2)a+(-5.2)b+(-53.0)c+(-85.3)d+(-80.1)e+(-

35.9)f+(-207.7)g+(46.1)h+(-344.4)Iln $[P(CMS3)/P(CMS1)]$ =282.0+(-91.0)a+(-4.5)b+(-52.4)c+(-83.7)d+(-78.9)e+(-32.2)f+(-141.9)g+(43.1)h+(-173.5)I; ln $[P(CMS4)/P(CMS1)]$ =283.9+(-92.1)a+(-5.9)b+(-50.9)c+(-83.7)d+(-80.2)e+(-35.2)f+(-143.8)g+ (47.7)h+(-366.0)I; a=TFF3 (0:H-score≥10, 1:H-score<10), b=SPINK4 (0:H-score<20, 1:H-score≥20), c=KIT(0:absent, 1: present), d=CDX2(0:H-score≥150, 1:H-score<150), e=ZMYND8(0:low, 1: high), f=MUC2(0:H-score<10, 1:H-score≥10), g=MUC5AC(0:H-score<10, 1:H-score≥10), h=SNAI1(0:H-score<20, 1:H-score≥20), i=MSI status(0:MSS/MSI-low, 1:MSI-High).

For NMF classification, NMF1 was selected as reference. ln $[P(NMF2)/P(NMF1)]$ =-1.33+(0.34)a+(-2.09)b+(-0.55)c+(0.94)d+(1.51)e+(-0.79)f+(1.89)g+(2.52)h+(2.55)I; ln $[P(NMF3)/P(NMF1)]$ = (-0.4)+(2.05)a+(-2.34)b+(-1.61)c+(1.07)d+(1.8)e+(-0.91)f+(-0.61)g+(-15.8)h+(0.45)I; ln $[P(NMF4)/P(NMF1)]$ =3.18+(1.31)a+(-2.39)b+(-2.96)c+(-0.39)d+(0.61)e+(-1.42)f+(-1.22)g+(-19.76)h+(-14.58)I; a=SNAI1(0:H-score<20, 1:H-score≥20), b=MUC2(0:H-score<10, 1:H-score≥10), c=SPINK4 (0:H-score<20, 1:H-score≥20), d=HTR2B(0:H-score<100, 1:H-score≥100), e= CDX2(0:H-score≥150, 1:H-score<150), f=ZMYND8(0:low, 1: high), g=TFF3 (0:H-score≥10, 1:H-score<10), h= MSI status(0:MSS/MSI-low, 1:MSI-High), i=MUC5AC(0:H-score<10, 1:H-score≥10). From above equations, we calculated the predictive probabilities for CMS and NMF classification.

**13. Statistical analysis**

Statistical analysis was performed to analyze associations of mutation, protein expression and gene copy number status with clinical characteristics using Pearson's Chi square and Fisher's exact test. The Kaplan–Meier method was used to estimate the survival rates for different groups. The equivalences of the survival curves were tested by log-rank statistics. The Cox proportional hazards model was employed for univariate and multivariate survival analyses. Those variables, being statistically significant found in the univariate survival analysis, were evaluated in the multivariate survival analysis. All results with a two-sided p-value < 0.05 were

considered significant. Statistical calculations were performed using the statistical package SPSS 21.0 (IBM Corp., Armonk, NY).

### 14. Ethical compliance

The institutional review board of Severance Hospital, Yonsei University, Seoul, Korea, approved this retrospective study following the ethical guidelines and the Declaration of Helsinki. A separate human body derivative donation consent form was obtained.

## III. RESULTS

### 1. Clinicopathologic features of the CRC patients

Patient cohort 1, the training cohort, consisted of 101 stage III CRCs treated with the FOLFOX regimen as adjuvant chemotherapy. Cohort 2, the validation cohort, consisted of 401 CRCs from stage I to stage IV. The clinicopathologic characteristis are shown in Table 3. Because of the larger proportion of advanced stages in cohort 1 compared to cohort 2, the CRCs in cohort 1 showed larger tumor size and more infiltrative invasion patterns. The mean patient age was younger in cohort 1 than in cohort 2.

The brief study design is shown in Figure 2. Using cohort 1, I analyzed the mRNA gene expression profiles and classified the CRCs into molecular subtypes. I then identified and selected the subtype specific gene markers to develop the IHC classifiers. After creating the IHC classifier models, I adjusted cohort 2 into the IHC classifier models and evaluated the clinicopathologic characteristics and outcomes.

**Table 3. Clinicopathologic features of the CRC patients of cohort 1 and cohort 2**

| Category | Variable | Cohort 1 (n=101) | | Cohort 2 (n=401) | | p-value |
|---|---|---|---|---|---|---|
| Age, years | | 58.98±11.17 | | 62.21±11.92 | | 0.014 |
| Sex | Male | 51 | 50.50% | 243 | 60.60% | 0.071 |
| | Female | 50 | 49.50% | 158 | 39.40% | |
| Location | Right side | 36 | 35.64% | 186 | 46.38% | 0.057 |
| | Left side | 65 | 64.36% | 215 | 53.62% | |
| Preop CEA level | ≤5ng/ml | 73 | 72.28% | 276 | 68.83% | 0.547 |
| | >5ng/ml | 28 | 27.72% | 125 | 31.17% | |
| Gross type | Exophytic | 77 | 76.24% | 298 | 74.31% | 0.798 |
| | Non exophytic | 24 | 23.76% | 103 | 25.69% | |
| Size, cm | | 5.11±1.96 | | 4.68±2.27 | | 0.06 |
| Differentiation | Well | 5 | 4.95% | 13 | 3.24% | 0.581 |
| | Moderately | 89 | 88.12% | 355 | 88.53% | |
| | Poorly | 7 | 6.93% | 33 | 8.23% | |
| Mucin formation | Absent | 72 | 71.29% | 303 | 75.56% | 0.4 |
| | Focal | 25 | 24.75% | 76 | 18.95% | |
| | Predominant | 4 | 3.96% | 22 | 5.49% | |
| Crohn like lymphoid reaction | low-density | 68 | 67.33% | 272 | 67.83% | 0.906 |
| | high-density | 33 | 32.67% | 129 | 32.17% | |
| Invasion pattern | expending | 15 | 14.85% | 112 | 27.93% | 0.007 |
| | infiltrative | 86 | 85.15% | 289 | 72.07% | |

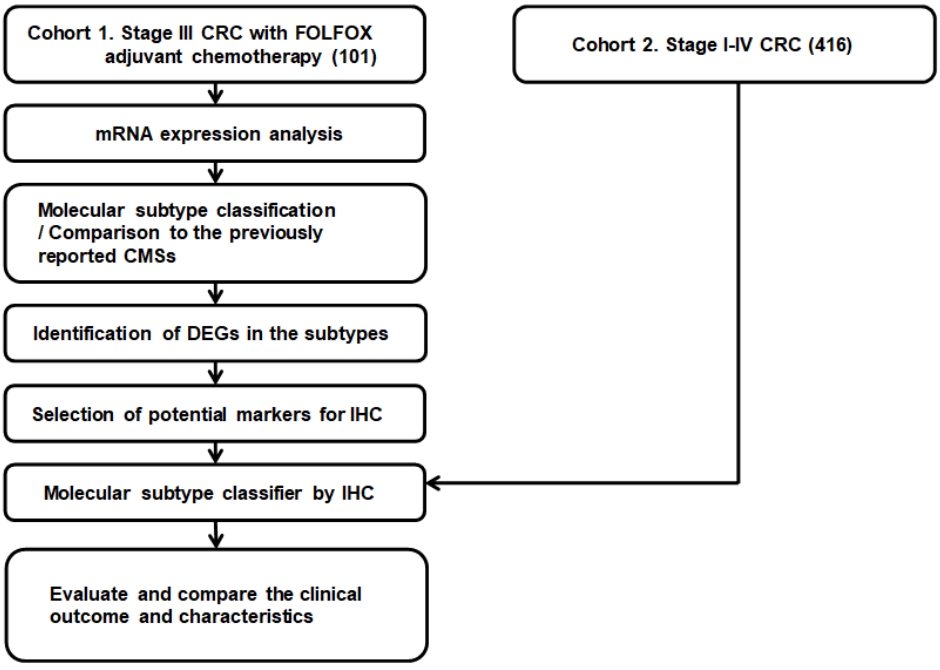


**Figure 2. Study design.** A total of 101 CRC tissue specimens in the cohort 1 was evaluated for molecular classification and IHC molcular subtype classifier and cohort 2 was validated using IHC molecular subtype classifier.

**2. Unsupervised clustering analysis of mRNA expression profiles identifies four distinct molecular subtypes**

I determined the mRNA expression profiles of cohort 1 by microarray analysis of 101 CRCs and 35 non-neoplastic colon mucosa tissue samples, using the Human HT-12 v4 Expression BeadChip (Illumina, Inc., San Diego, CA, USA), which contains 47,323 probes representing 31,332 annotated genes. I identified 4,823 genes as differentially expressed genes (DEGs) that displayed a |fold change|>2 and P-value<0.05 in colon cancers, as compared to non-neoplastic colon mucosa. To further analyze colon cancer-specific gene expression, I used unsupervised hierarchical clustering analysis of the 4,823 DEGs and found that CRC samples grouped into four separate clusters, distinct from the non-neoplastic colon mucosa tissues (Figure 3). These gene expression microarray data have been deposited in

NCBI's Gene Expression Omnibus (GEO) database (http://www.ncbi.nlm.nih.gov/geo/) and are accessible through the GEO Series accession number GSE83889.

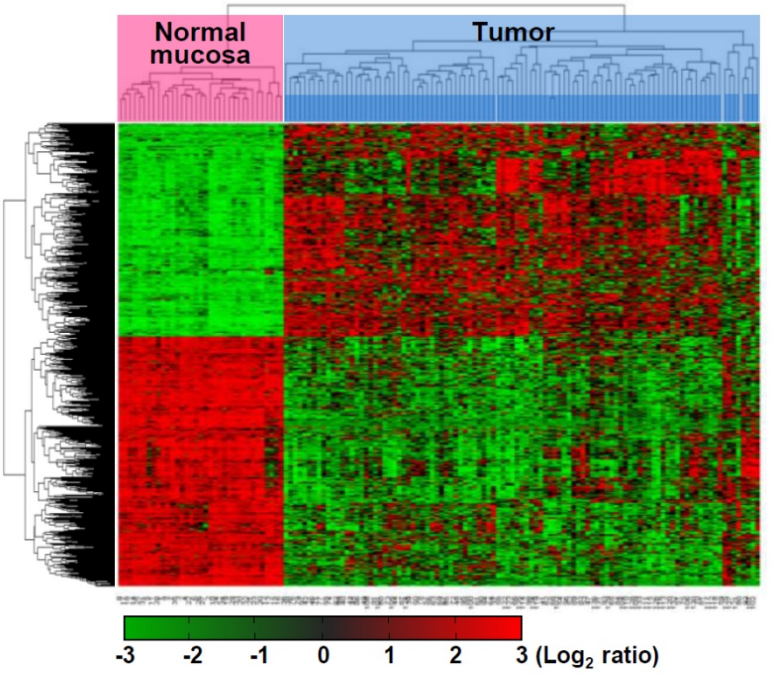


**Figure 3. Unsupervised hierarchical clustering analysis of mRNA expression profiles from colon cancer tissue.** Unsupervised classification identifies four distinct molecular subtypes. Red and green colors indicate transcript levels above and below the sample median, respectively. Complete separation of 35 normal colon tissues (red) and 101 colon cancers (sky blue) was evident based on gene expression profiles.

**3. Gene expression-based molecular subtypes are categorized into four groups by nonnegative matrix factorization**

To classify the 101 colorectal tumors of cohort 1 according to the gene profiles of those tumors, I performed NMF consensus clustering using 1,764 tumor-specific DEGs that displayed a |fold change|>2 and P-value<0.01 in a stricter condition compared to non-neoplastic tissues. NMF is a nonnegative matrix factorization algorithm that focuses on the analysis of data matrices comprising non-negative elements. To identify high consensus clusters (cophenetic coefficient, ρk, is closer to 1.0), I applied various conditions for the factorization algorithm for each value of k cluster (k=2, 3, 4, 5, 6, and 7). I then obtained a consensus plot and cophenetic coefficient for each k=2 to 7 value and selected k values with high consensus. Using this consensus analysis with the 1,764 DEGs, I obtained good consensus for k = 4 clusters (coph=0.8961), providing evidence for the existence of four consensus clusters (type 1) and hence, four functional distinct properties that can be elucidated from the DEGs of 101 colorectal tumors; group 1 (n=22, 21.8%), group 2 (n=21, 20.8%), group 3 (n=16, 15.8%), and group 4 (n=42, 41.6%) (Figure 4A). The consensus matrix showed that groups 1 and 4 appeared as individualized clusters (sharp consensus clustering), whereas groups 2 and 3 showed less distinct boundaries.

I also performed NMF consensus clustering with another selected gene set; the 1,538 DEGs that demonstrated differential expression among tumor groups were divided by the hierarchical clustering method when |fold change|>2 and P-value<0.01. In the NMF consensus analysis with these 1,538 DEGs, there were k = 4 clusters (type 2) with high cophenetic coefficient (coph=0.8612); group 1 (n=20, 19.8%), group 2 (n=29, 28.7%), group 3 (n=24, 23.8%), and group 4 (n=28, 27.7%) (Figure 4B). Samples represented in each group divided by NMF with either the 1,764 or the 1,538 DEGs were similar (77.2% matched).

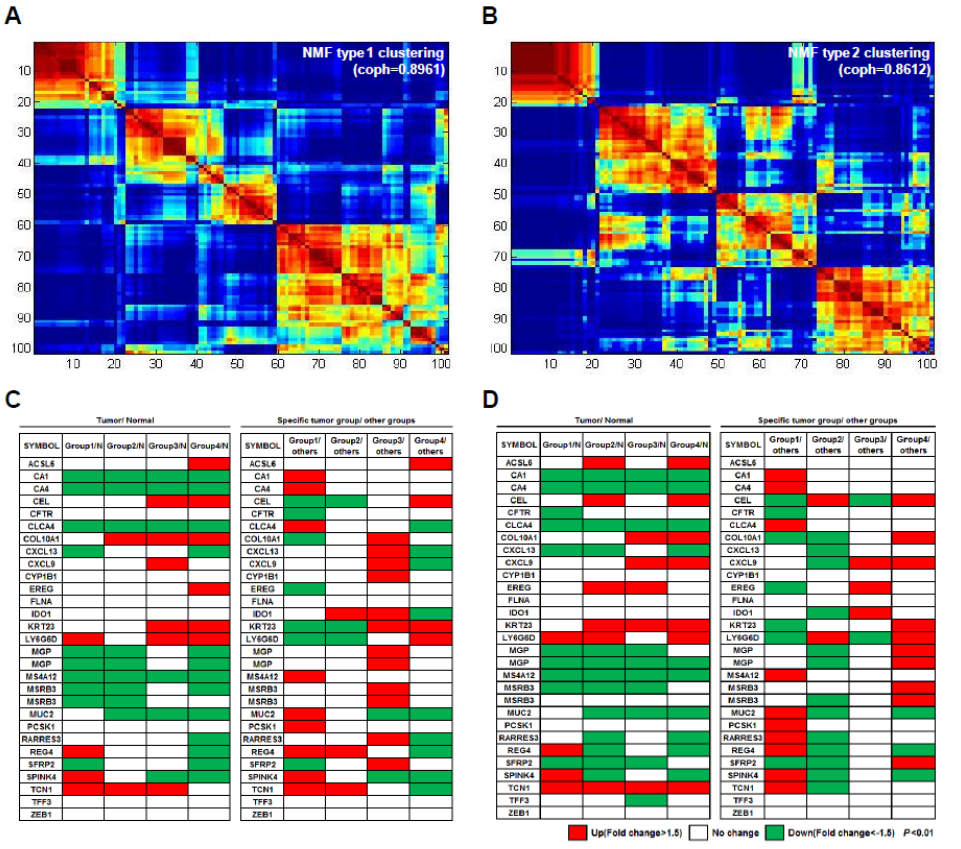


**Figure 4. Four molecular subtypes identified using consensus clustering based NMF** (A) NMF type 1 clustering: consensus clustering using 1,764 DEGs in tumors compared to non-neoplastic tissues. (B) NMF type 2 clustering: clustering with 1,538 DEGs specific for one group, as compared to other tumor groups. (C and D) Analysis of the mRNA expression patterns of the 30 genes from the CRCassigner-30 was performed according to each of the four subtypes from NMF type 1 clustering (C) and NMF type 2 clustering (D). NMF type 1 clustering showed more distinct gene expression patterns between the tumor subtypes than that of the NMF type 2 clustering.

To further characterize the gene expression of the different tumor subtypes, I analyzed expression patterns of 30 genes comprising a colon cancer classification system, known as the CRC assigner-30 [17], in four subtypes that were obtained from each of type 1 and type 2 clustering under the conditions of |fold change|>1.5 and P-value<0.01 (Figure 4C, 4D). In the four tumor groups obtained from type 1 clustering, the expression of 5 genes was found to have increased in a specific tumor group, compared to the normal group (left panel of Figure 4C). In addition, the expression of 18 genes was found to have increased in a specific tumor group, compared to the rest of the tumor groups (right panel of Figure 4C). In the four tumor groups obtained from type 2 clustering, the expression of two and 17 genes was also found to have increased in a specific tumor group compared to the normal group or the rest of the tumor groups, respectively (Figure 4D). Overall, type 1 clustering (NMF with 1,764 DEGs in tumors compared to non-neoplastic tissues) showed more distinct gene expression patterns among tumor groups than did those of type 2 clustering (NMF with 1,538 DEGs in tumor groups divided by unsupervised hierarchical clustering). Therefore, I selected type 1 clustering for the subsequent gene expression analyses.

**4. Correlation between NMF based subtypes and CMS**

I next employed 'CMS classifier' (scripts and code for CMS classifier available at: https://github.com/Sage-Bionetworks/crcsc) for CMS classification [17,18] of our 101 CRC samples. Among the 101 samples, 80 tumors were representative of each CMS; whereas, the remaining 21 unlabeled samples (non-consensus samples) did not have any consistent pattern within the four CMS groups. I compared the CMS grouping with our subtypes, and found that, of the 101 cancers, 63 showed a close correlation to one of the four subtypes (Table 4).

**Table 4. Correlation between NMF-based groups and CMS subtypes**

| | | NMF-based group | | | | Total |
|---|---|---|---|---|---|---|
| | | Group 2 | Group 4 | Group 1 | Group 3 | |
| CMS | CMS1 | 10(66.6%) | 0(%) | 0(0%) | 0(0%) | 10 |
| | CMS2 | 4(26.7%) | 31(79.5%) | 3(18.8%) | 0(0%) | 38 |
| | CMS3 | 1(6.7%) | 0(0%) | 12(75%) | 0(0%) | 13 |
| | CMS4 | 0(0%) | 8(20.5%) | 1(6.2%) | 10(100%) | 19 |
| | Indetermined | 6 | 3 | 6 | 6 | 21 |
| | Total | 21 | 42 | 22 | 16 | 101 |

Specifically, 10 of 21 group 2 samples were included in CMS1 (microsatellite instability immune and characterized as hypermutated, microsatellite unstable and strong immune activation), and all ten that were grouped in CMS1 were also classified in group 2. Similarly, 31 out of 42 samples from group 4 were classified as CMS2 (canonical and characterized by marked WNT and MYC signaling activation), while 31 out of 38 samples in CMS2 were also found in group 4. I further observed that 12 out of 22 group 1 samples were classified as CMS3 (metabolic and characterized by evident metabolic dysregulation), and 12 out of 13 CMS3 cases belonged to group 1. Finally, I found that ten out of 16 samples belonging to group 3 were classified into CMS4 (mesenchymal and characterized by prominent transforming growth factor activation, stromal invasion and angiogenesis), while 10 out of 19 CMS4 samples also belonged to group 3. When I excluded the 21 non-consensus cases, a 79% correlation (63 out of 80 cases) was found between the CMS classification and our molecular classification.

### 5. Clinicopathologic characteristics of CRCs according to molecular subtypes

I compared several clinicopathologic and molecular characteristics according to the CMSs, with the except for the indeterminate cases (Table 5). I found that clinicopathologic parameters were showing significant differences among CMSs. Specifically, differences in tumor location ($P = 0.004$), mucin formation ($P < 0.001$), Crohn-like reaction ($P = 0.029$), invasion pattern ($P = 0.012$), TSP ($P = 0.041$), GMS ($P = 0.017$), immunoscore ($P < 0.001$), and proportion of microsatellite instability (MSI-High) ($P < 0.001$) were remarkable. Tumor location

was predominantly on the right side in CMS1, while the other subtypes showed left-sided tumor location dominantly. Mucinous adenocarcinoma (> 50% of extracellular mucin formation) was observed in CMS3 and CMS4. In CMS1, Crohn-like reaction (60%), high immunoscore and expanding invasion pattern (50%) were more frequently found than in the other types. High TSP, low KM grade, and GMS2 were characteristic of CMS4. I also found significant differences in several parameters among the NMF-based groups. Specifically, there were significant differences in tumor location (P=0.001), mucin formation (P<0.001), Tumor stroma percentage (TSP) (P=0.018), Klintrap-Makinen (KM) grade (P=0.018), Glasgow Microenvironment Score (GMS) (P=0.012), immunoscore (P=0.002), incidence of KRAS mutation (P=0.01), and proportion of microsatellite instability (MSI-High) (P=0.001), Further, >50% of the cancers in groups 3 (62.5%) and 4 (85.7%) presented as left-sided tumors. Conversely, >50% of the cancers in groups 2 (57.1%) were located on the right side. Histologically, most tumors were adenocarcinomas with moderate differentiation; there were four mucinous adenocarcinomas (>50% of extracellular mucin formation) and all of these were included in group 1. With respect to the extracellular mucin production, most tumors in groups 3 (87.5%) and 4 (92.9%) did not demonstrate extracellular mucin production, whereas, >50% of tumors in groups 1 and 2 showed extracellular mucin production. About half of the cancers in group 3 had high tumor stroma percentage (TSP), while the other groups showed predominantly low TSP. High KM grade was found in nearly all cases (95.24%) in group 2, and high immunoscore was observed in group 2 and group 3. About 30% of group 3 tumors had the features of GMS2, weak KM grade, and high TSP. I also found frequent KRAS mutations in group 1 (63.6%) and group 3 (56.3%) and less frequent mutation in groups 2 (28.6%) and 4 (26.2%). Further, I observed MSI-High in groups 2 (28.6%), and group 1 (9%), but no instances in groups 3 and 4. The Crohn-like lymphoid reaction is a common feature of MSI-High in colon cancer, and therefore, this was evaluated using the Väyrynen-Mäkinen criteria. However, no significant differences were found with respect to these criteria among the different subtypes.

**Table 5. Clinicopathologic features of cohort 1 according to the CMS subtype**

| Category | Variable | CMS 1 n=10, 9.9% | | CMS 2 n=38, 37.6% | | CMS 3 n=13, 12.9% | | CMS 4 n=19, 18.8% | | p-value |
|---|---|---|---|---|---|---|---|---|---|---|
| Age, years | | 51.1±15.15 | | 59.08±11.33 | | 61±9.69 | | 60.53±9.82 | | 0.337 |
| Sex | Male | 4 | 40.00% | 22 | 57.90% | 9 | 69.20% | 9 | 47.40% | 0.467 |
| | Female | 6 | 60.00% | 16 | 42.10% | 4 | 30.80% | 10 | 52.60% | |
| Location | Right side | 7 | 70.00% | 6 | 15.80% | 6 | 46.20% | 8 | 42.10% | 0.004 |
| | Left side | 3 | 30.00% | 32 | 84.20% | 7 | 53.80% | 11 | 57.90% | |
| Preop CEA level | ≤5ng/ml | 10 | 100.00% | 26 | 68.40% | 11 | 84.60% | 15 | 78.90% | 0.189 |
| | >5ng/ml | 0 | 0.00% | 12 | 31.60% | 2 | 15.40% | 4 | 21.10% | |
| Gross type | Exophytic | 10 | 100.00% | 27 | 71.10% | 11 | 84.60% | 14 | 73.70% | 0.24 |
| | Non exophytic | 0 | 0.00% | 11 | 28.90% | 2 | 15.40% | 5 | 26.30% | |
| Size(cm) | | 6.36±2.42 | | 4.88±1.66 | | 4.93±2.40 | | 4.62±1.32 | | 0.239 |
| Differentiation | Well | 0 | 0.00% | 3 | 7.89% | 1 | 7.69% | 1 | 5.26% | 0.146 |
| | Moderately | 7 | 70.00% | 34 | 89.47% | 12 | 92.31% | 16 | 84.21% | |
| | Poorly | 3 | 30.00% | 1 | 2.63% | 0 | 0.00% | 2 | 10.53% | |
| Mucin formation | Absent | 4 | 40.00% | 34 | 89.50% | 6 | 46.20% | 17 | 89.50% | <0.001 |
| | Focal | 6 | 60.00% | 4 | 10.50% | 6 | 46.20% | 1 | 5.30% | |
| | Predominant(>50%) | 0 | 0.00% | 0 | 0.00% | 1 | 7.70% | 1 | 5.30% | |
| Crohn like lymphoid reaction | Low-density group | 4 | 40.00% | 31 | 81.60% | 7 | 53.80% | 11 | 57.90% | 0.029 |
| | High-density group | 6 | 60.00% | 7 | 18.40% | 6 | 46.20% | 8 | 42.10% | |
| Invasion pattern | Expending | 5 | 50.00% | 5 | 13.20% | 0 | 0.00% | 2 | 10.50% | 0.012 |
| | Infiltrative | 5 | 50.00% | 33 | 86.80% | 13 | 100.00% | 17 | 89.50% | |
| Lymphovascular invasion | Absent | 4 | 40.00% | 17 | 44.70% | 6 | 46.20% | 10 | 52.60% | 0.938 |
| | Present | 6 | 60.00% | 21 | 55.30% | 7 | 53.80% | 9 | 47.40% | |
| Tumor budding | Absent | 3 | 30.00% | 6 | 15.79% | 2 | 15.38% | 1 | 5.26% | 0.543 |
| | Low | 6 | 60.00% | 21 | 55.26% | 6 | 46.15% | 11 | 57.89% | |
| | High | 1 | 10.00% | 11 | 28.95% | 5 | 38.46% | 7 | 36.84% | |
| TSP | Low | 10 | 100.00% | 32 | 84.21% | 10 | 76.92% | 11 | 57.89% | 0.041 |

| | | | | | | | | | | |
|---|---|---|---|---|---|---|---|---|---|---|
| | High | 0 | 0.00% | 6 | 15.79% | 3 | 23.08% | 8 | 42.11% | |
| KM grade | Low | 0 | 0.00% | 13 | 34.21% | 3 | 23.08% | 8 | 42.11% | 0.078 |
| | High | 10 | 100.00% | 25 | 65.79% | 10 | 76.92% | 11 | 57.89% | |
| | GMS 0 | 10 | 100.00% | 25 | 65.79% | 10 | 76.92% | 11 | 57.89% | 0.017 |
| GMS | GMS1 | 0 | 0.00% | 10 | 26.32% | 2 | 15.38% | 1 | 5.26% | |
| | GMS2 | 0 | 0.00% | 3 | 7.89% | 1 | 7.69% | 7 | 36.84% | |
| Immunoscore | Low | 2 | 20.00% | 23 | 60.53% | 6 | 46.15% | 10 | 52.63% | <0.001 |
| | Intermediate | 0 | 0.00% | 14 | 36.84% | 5 | 38.46% | 5 | 26.32% | |
| | High | 8 | 80.00% | 1 | 2.63% | 2 | 15.38% | 4 | 21.05% | |
| BRAF | Wild type | 9 | 90.00% | 38 | 100.00% | 13 | 100.00% | 19 | 100.00% | 0.125 |
| | Mutation | 1 | 10.00% | 0 | 0.00% | 0 | 0.00% | 0 | 0.00% | |
| KRAS | Wild type | 8 | 80.00% | 27 | 71.10% | 5 | 38.50% | 13 | 68.40% | 0.149 |
| | Mutation | 2 | 20.00% | 1 | 28.90% | 8 | 61.50% | 6 | 31.60% | |
| MSI status | MSS/MSI-low | 4 | 40.00% | 38 | 100.00% | 12 | 92.31% | 19 | 100.00% | <0.001 |
| | MSI-High | 6 | 60.00% | 0 | 0.00% | 1 | 7.69% | 0 | 0.00% | |

TSP:Tumor stroma percentage, KM grade: Klintrap-Makinen grade, GMS: Glasgow microenvironment score, MSS: Microsatellite stability, MSI: Microsatellite instability

**Table 6. Clinicopathologic features according to the NMF molecular subtype**

| Category | Variable | Group 1 n=22, 21.8% | | Group 2 n=21,20.8% | | Group 3 n=16, 15.8% | | Group 4 n=42, 41.6% | | p-value |
|---|---|---|---|---|---|---|---|---|---|---|
| Age, years | | 57.95±13.26 | | 58.09±13.67 | | 62±9.04 | | 58.81±9.42 | | 0.802 |
| Sex | Male | 14 | 63.60% | 8 | 38.10% | 7 | 43.80% | 22 | 52.40% | 0.376 |
| | Female | 8 | 36.40% | 13 | 61.90% | 9 | 56.20% | 20 | 47.60% | |
| Location | Right side | 12 | 54.50% | 12 | 57.10% | 6 | 37.50% | 6 | 14.30% | <0.001 |
| | Left side | 10 | 45.50% | 9 | 42.90% | 10 | 62.50% | 36 | 85.70% | |
| PreOP CEA level | ≤5ng/ml | 18 | 81.80% | 17 | 81.00% | 10 | 62.50% | 28 | 66.70% | 0.367 |
| | >5ng/ml | 4 | 18.20% | 4 | 19.00% | 6 | 37.50% | 14 | 33.30% | |
| Gross type | Exophytic | 20 | 90.91% | 18 | 85.71% | 11 | 68.75% | 28 | 66.67% | 0.102 |
| | Non exophytic | 2 | 9.09% | 3 | 14.29% | 5 | 31.25% | 14 | 33.33% | |
| Size (cm) | | 5.5±2.535 | | 5.79±2.197 | | 5.01±1.224 | | 4.6±1.609 | | 0.171 |
| Differentiation | Well | 2 | 9.09% | 0 | 0.00% | 1 | 6.25% | 2 | 4.76% | 0.507 |
| | Moderately | 20 | 90.91% | 18 | 85.71% | 14 | 87.50% | 37 | 88.10% | |
| | Poorly | 0 | 0.00% | 3 | 14.29% | 1 | 6.25% | 3 | 7.14% | |
| Mucin formation | Absent | 10 | 45.50% | 9 | 42.80% | 14 | 87.50% | 39 | 92.90% | <0.001 |
| | Focal | 8 | 36.40% | 12 | 57.20% | 2 | 12.50% | 3 | 7.10% | |
| | Predominant(>50%) | 4 | 18.20% | 0 | 0.00% | 0 | 0.00% | 0 | 0.00% | |
| Crohn like lymphoid reaction | Low-density group | 14 | 63.60% | 13 | 61.90% | 8 | 50.00% | 33 | 78.60% | 0.157 |
| | High-density group | 8 | 36.40% | 8 | 38.10% | 8 | 50.00% | 9 | 21.40% | |
| Invasion pattern | Expending | 2 | 9.10% | 7 | 33.30% | 2 | 12.50% | 4 | 9.50% | 0.098 |
| | Infiltrative | 20 | 90.90% | 14 | 66.70% | 14 | 87.50% | 38 | 90.50% | |
| Lymphovascular invasion | Absent | 12 | 54.55% | 10 | 47.62% | 8 | 50.00% | 18 | 42.86% | 0.847 |
| | Present | 10 | 45.45% | 11 | 52.38% | 8 | 50.00% | 24 | 57.14% | |
| Tumor budding | Absent | 5 | 22.73% | 3 | 14.29% | 1 | 6.25% | 5 | 11.90% | 0.901 |
| | Low | 11 | 50.00% | 11 | 52.38% | 10 | 62.50% | 23 | 54.76% | |
| | High | 6 | 27.27% | 7 | 33.33% | 5 | 31.25% | 14 | 33.33% | |
| TSP | Low | 18 | 81.82% | 19 | 90.48% | 8 | 50.00% | 36 | 85.71% | 0.018 |
| | High | 4 | 18.18% | 2 | 9.52% | 8 | 50.00% | 6 | 14.29% | |

| | | | | | | | | | | |
|---|---|---|---|---|---|---|---|---|---|---|
| KM grade | Low | 6 | 27.27% | 1 | 4.76% | 6 | 37.50% | 18 | 42.86% | 0.018 |
| | High | 16 | 72.73% | 20 | 95.24% | 10 | 62.50% | 24 | 57.14% | |
| GMS | GMS 0 | 16 | 72.73% | 20 | 95.24% | 10 | 62.50% | 24 | 57.14% | 0.012 |
| | GMS1 | 4 | 18.18% | 1 | 4.76% | 1 | 6.25% | 12 | 28.57% | |
| | GMS2 | 2 | 9.09% | 0 | 0.00% | 5 | 31.25% | 6 | 14.29% | |
| Immunoscore | Low | 14 | 63.64% | 7 | 33.33% | 5 | 31.25% | 27 | 64.29% | 0.002 |
| | Intermediate | 6 | 27.27% | 5 | 23.81% | 4 | 25.00% | 13 | 30.95% | |
| | High | 2 | 9.09% | 9 | 42.86% | 7 | 43.75% | 2 | 4.76% | |
| BRAF | Wild type | 22 | 100.00% | 20 | 95.20% | 16 | 100.00% | 42 | 100.00% | 0.366 |
| | Mutation | 0 | 0.00% | 1 | 4.80% | 0 | 0.00% | 0 | 0.00% | |
| KRAS | Wild type | 8 | 36.40% | 15 | 71.40% | 7 | 43.80% | 31 | 73.80% | 0.01 |
| | Mutation | 14 | 63.60% | 6 | 28.60% | 9 | 56.30% | 11 | 26.20% | |
| MSI status | MSS/MSI-low | 20 | 90.91% | 15 | 71.43% | 16 | 100.00% | 42 | 100.00% | 0.001 |
| | MSI-High | 2 | 9.09% | 6 | 28.57% | 0 | 0.00% | 0 | 0.00% | |

TSP:Tumor stroma percentage, KM grade: Klintrap-Makinen grade, GMS: Glasgow microenvironment score, MSS: Microsatellite stability, MSI: Microsatellite instability

Five histologic features were identified: complex tubular, papillary, serrated, solid, and desmoplastic. The common histologic features were identified according to the molecular subtypes (Figure 5). The complex tubular pattern was most frequently found in all of the subtypes. Besides the complex tubular pattern, in group 1 and CMS 3, the papillary and serrated features were commonly found, while in group 2 and CMS 1, the solid feature was characteristic. In group3 and CMS4, the desmoplastic feature was largely noted, and in group 4 and CMS 2, the papillary and desmoplastic features were observed next to the complex tubular feature.

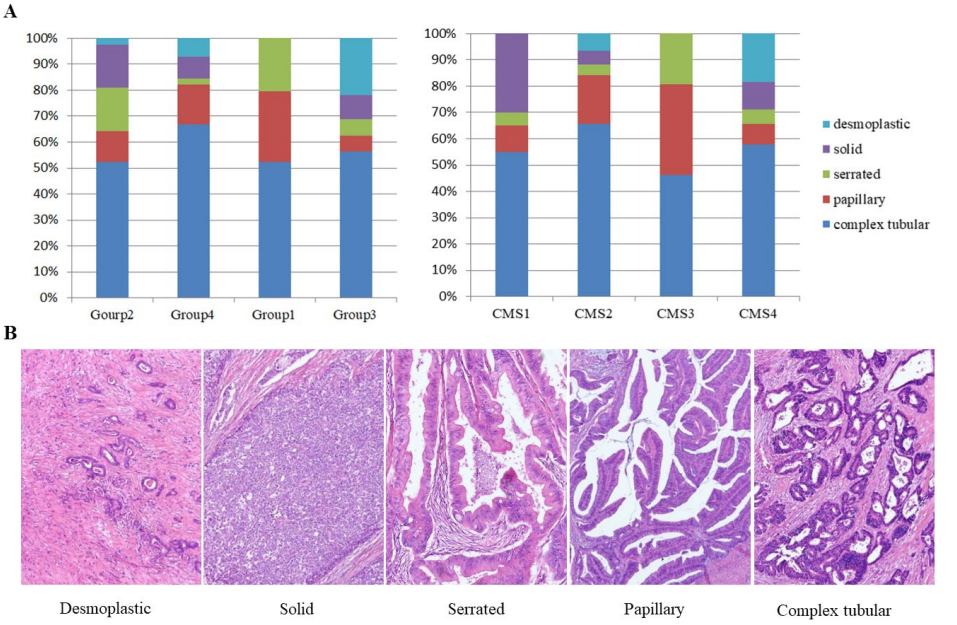


**Figure 5. Histologic features according to the molecular subtypes** (A) Major histologic features of each subtypes according to the NMF based classification and CMS classification. (B) Representative image of the five histologic features; desmoplastic, solid, serrated, papillary, and complex tubular pattern.

**6. Identification of subtype specific markers**

I further analyzed gene expression patterns to identify gene subsets that are differentially expressed in the four groups, as compared to neoplastic colon mucosa tissues and/or other groups. Differently expressed genes were identified in each group: 194 genes in group 1; 736 genes in group 2; 493 genes in group 3; and 634 genes in group 4. In addition, 275 genes, 372 genes, 558 genes, and 184 genes were differentially expressed in each respective group, as compared to the other groups. I next selected genes characteristic of each group by choosing those that are differentially regulated as compared to both normal tissue and the other molecular groups. I accordingly identified 292 genes as potential group markers (Figure 6A, 6B). I finally selected ten genes from this group that are overexpressed >1.5 fold in one group, as compared to both normal tissues and tumors in other groups. Among these genes, DEFA5, DUOX2, KLK12, and ALDOB in group 1, CCDC58, MOCOS, and FAM81A in group 2, HOPX, TAGLN, GREM1, THBS4, COL3A1, PRRX1, RAB31, MYL9, CTSK, and SPARC in group 3, and DSC3 and CAB39L in group 4 were particularly up-regulated (> 2.0-fold) (Figure 6C).

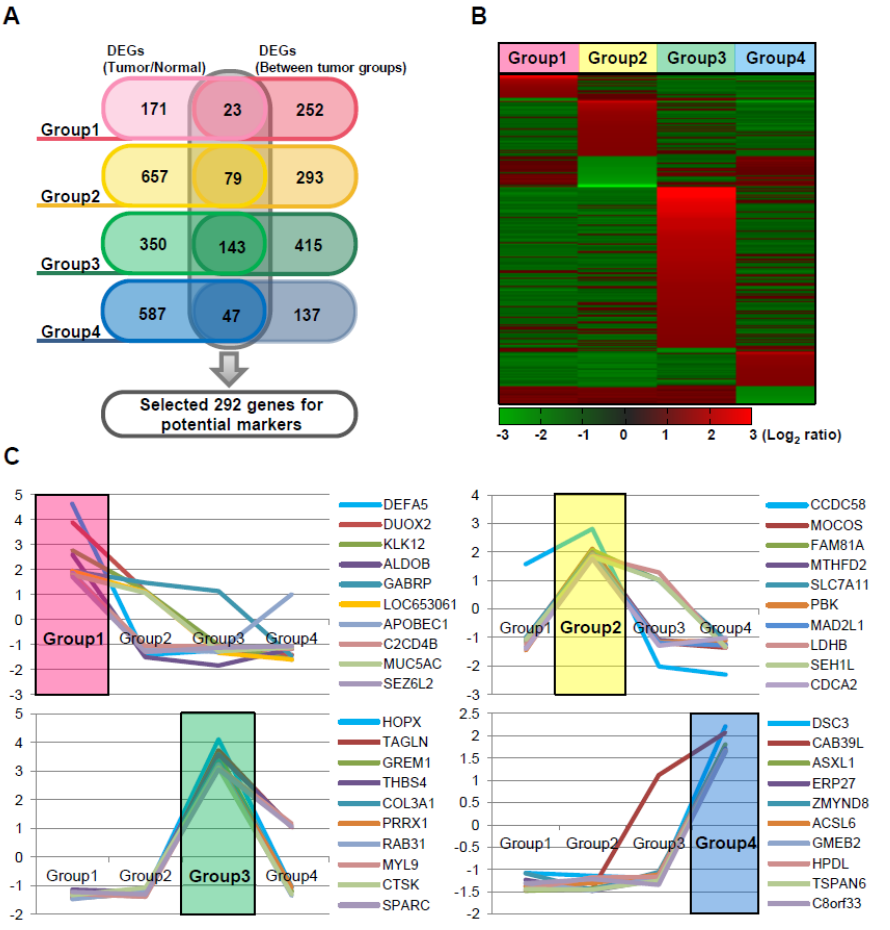


**Figure 6. Identification of mRNAs differentially expressed in each of the four groups, as compared to non-neoplastic colon mucosa tissue and/or the other groups.** (A) Venn diagram showing a total of 292 potential marker genes, with group specific upregulation. (B) Heatmap of the mRNA expression profiles of these 292 DEGs according to the four molecular groups. (C) The mRNA expression profiles of ten selected genes from each group.

**7. Establishment of IHC subtype classifier to predict molecular subtype**

I separately tried to establish the IHC classifier models that can predict molecular subtypes. To design the IHC classifier, I used the IHC expression data of 101 cases for the NMF-based group and that of 80 cases for CMSs, except for the indeterminate cases. The accuracy and the AIC value of all possible IHC classifiers are shown in Figure 7. Regarding discriminatory ability, a high accuracy value was considered the better model. Furthermore, the AIC value represented a better model for discriminatory ability. The accuracy was increased as the number of combined markers was increased. The mean accuracy was about 0.55 when only two markers were used in combination, compared to a mean accuracy of 0.79 when ten markers were used. The mean AIC was the same, in reverse; when the number of combined markers was increased, the AIC decreased. I selected the IHC classifier showing high accuracy and low AIC value (Table 7). Nine factors were selected to predict CMS: MUC2, CDX2, ZMYND8, SPINK4, KIT, MUC5AC, Snail, TFF3 and MSI status. The accuracy value was 0.825 (95% CI = 0.737 - 0.825) with an AIC value of 134.771 (95% CI = 134.507 - 160.549). CMS group with the highest predictive probability among four CMSs was selected as predicted CMS for each case. However, when we compared the predictive probability of molecular classifier and IHC classifier using the intraclass correlation coefficient (ICC), the average measures mean of the ICC was 0.18 (P = 0.219).

For NMF-based groups, I choose the nine following factors: SNAIl, MUC2, SPINK4, HTR2B, CDX2, ZMYND8, TFF3, MUC5AC, and MSI status. The accuracy (0.702, 95% confidence interval [CI] = 0.643 - 0.702) was high and AIC value was low (226.576, 95% CI = 226.576 - 237.358) than another marker combination.

**Table 7. The IHC classifiers to predict subtypes**

| | Predictive group | The number of factors | The combined factors | Accuracy (95% CI) | AIC (95% CI) |
|---|---|---|---|---|---|
| **The IHC classifier** | CMS | 9 | MUC2, CDX2, ZMYND8, MSI, SPINK4, KIT, MUC5AC, Snail, TFF3 | 0.825 (0.737-0.825) | 134.771 (134.507-160.549) |
| | NMF-based group | 9 | Snail, MUC2, SPINK4, HTR2B, CDX2, ZMYND8, TFF3, MSI, MUC5AC | 0.702 (0.643-0.702) | 226.576 (226.576-237.358) |

AIC: Akaike's Information Criterion

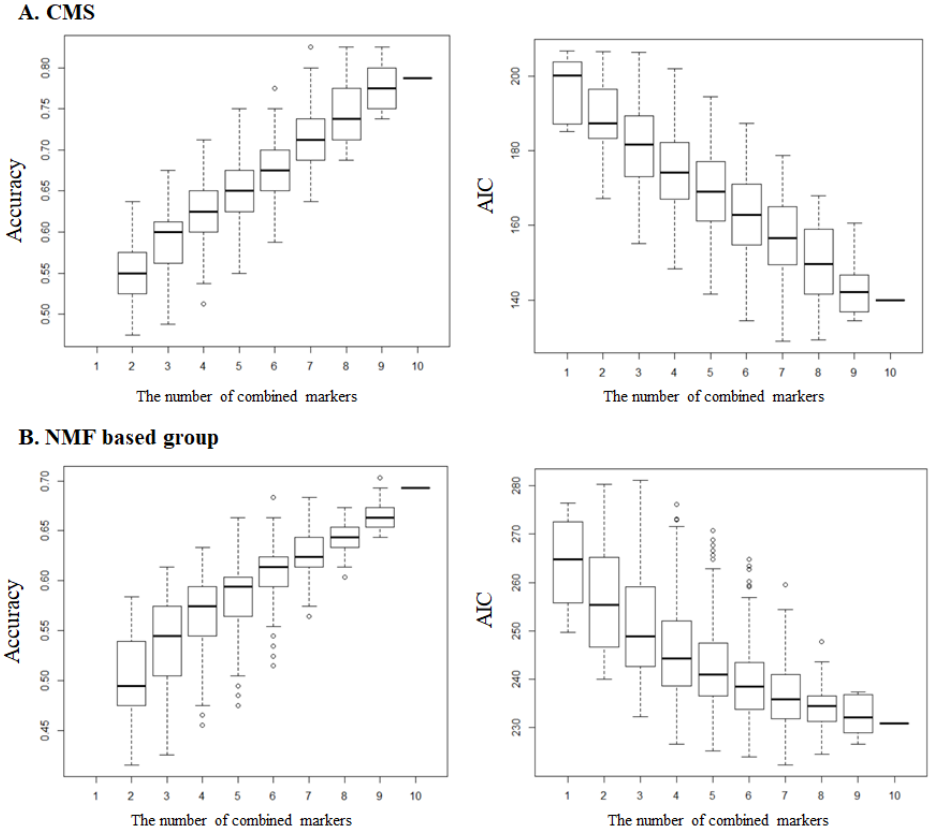


**Figure 7. Accuracy and AIC of the IHC classifiers** (A) Accuracy and AIC of the IHC classifiers to predict CMSs. (B) Accuracy and AIC of the IHC classifiers to predict NMF-based groups

**8. Similarities of the clinicopathologic characteristics of the predicted subtypes by IHC classifier and the molecular subtypes by transcriptome**

The predicted CMS in the validation cohort showed similar patterns of clinicopathologic characteristics to those of the training cohort (Table 8). Among 401 cases, 18.0% was classified as CMS1 (72 cases), 42.9% as CMS2 (172 cases), 19.2% as CMS3 (77 cases), and 20.0% as CMS4 (80 cases).

The factors showing significant differences similar to those of cohort 1 are following: tumor location ($P < 0.001$), mucin formation ($P < 0.001$), Crohn-like reaction ($P < 0.001$), invasion pattern ($P = 0.011$), TSP ($P \leq 0.001$), GMS ($P <$

0.001), and immunoscore (P = 0.001). Tumor location was predominantly on the right side in CMS1, while CMS2 and CMS4 left-sided tumor location was dominant. In CMS1, Crohn-like reaction (63.89%), along with high immunoscore (47.22%) and expanding invasion pattern (40.28%) were more frequently found than in the other types. High TSP, low KM grade, and GMS2 were also observed in CMS4, like those in cohort 1. Additional factors showed a remarkable difference among CMSs. Tumor sizes were larger in CMS1 and smaller in CMS4 (P < 0.001). In tumor differentiation, a large portion of poorly differentiated adenocarcinomas was included in CMS1 (P <0.001), while lymphovascular invasion and tumor budding was highly enriched in CMS4. In cohort 2, mucous adenocarcinoma (>50% of extracellular mucin formation) was mainly observed in CMS1, while this was observed in CMS3 and CMS4 in cohort 1. MSI-High was enriched in CMS1 (76.39%), and a small proportion was included in CMS3 (3.9%) which is known as mixed MSI subtype.

**Table 8. Clinicopathologic characteristics of the predicted CMS according to the IHC classifier**

| Category | Variable | CMS1 n=72, 18.0% | | CMS2 n=172, 42.9% | | CMS3 n=77, 19.2% | | CMS4 n=80, 20.0% | | *p*-value |
|---|---|---|---|---|---|---|---|---|---|---|
| Age, years | | 59.44±12.76 | | 62.69±10.76 | | 63.26±12.56 | | 61.66±12.25 | | 0.202 |
| Sex | Male | 46 | 63.89% | 108 | 62.79% | 44 | 57.14% | 45 | 56.25% | 0.636 |
| | Female | 26 | 36.11% | 64 | 37.21% | 33 | 42.86% | 35 | 43.75% | |
| Location | Right side | 58 | 80.56% | 49 | 28.49% | 41 | 53.25% | 38 | 47.50% | <0.001 |
| | Left side | 14 | 19.44% | 123 | 71.51% | 36 | 46.75% | 42 | 52.50% | |
| Preop CEA level | ≤5ng/ml | 54 | 75.00% | 114 | 66.28% | 57 | 74.03% | 51 | 63.75% | 0.298 |
| | >5ng/ml | 18 | 25.00% | 58 | 33.72% | 20 | 25.97% | 29 | 36.25% | |
| Gross type | Exophytic | 58 | 80.56% | 123 | 71.51% | 59 | 76.62% | 58 | 72.50% | 0.479 |
| | Non exophytic | 14 | 19.44% | 49 | 28.49% | 18 | 23.38% | 22 | 27.50% | |
| Size | | 5.93±2.74 | | 4.04±1.83 | | 4.55±2.09 | | 5.06±2.41 | | <0.001 |
| Differentiation | Well | 1 | 1.39% | 4 | 2.33% | 3 | 3.90% | 1 | 1.25% | <0.001 |
| | Moderately | 50 | 69.44% | 163 | 94.77% | 73 | 94.81% | 73 | 91.25% | |
| | Poorly | 21 | 29.17% | 5 | 2.91% | 1 | 1.30% | 6 | 7.50% | |
| Mucin formation | Absent | 32 | 44.44% | 163 | 94.77% | 43 | 55.84% | 65 | 81.25% | <0.001 |
| | Focal | 27 | 37.50% | 7 | 4.07% | 28 | 36.36% | 14 | 17.50% | |
| | Predominant >50%) | 13 | 18.06% | 2 | 1.16% | 6 | 7.79% | 1 | 1.25% | |
| Crohn like lymphoid reaction | Low-density group | 26 | 36.11% | 127 | 73.84% | 59 | 76.62% | 60 | 75.00% | <0.001 |
| | High-density group | 46 | 63.89% | 45 | 26.16% | 18 | 23.38% | 20 | 25.00% | |
| Invasion pattern | Expending | 29 | 40.28% | 36 | 20.93% | 20 | 25.97% | 27 | 33.75% | 0.011 |

| | | | | | | | | | | |
|---|---|---|---|---|---|---|---|---|---|---|
| | Infiltrative | 43 | 59.72% | 136 | 79.07% | 57 | 74.03% | 53 | 66.25% | |
| Lymphovascular invasion | Absent | 65 | 90.28% | 139 | 80.81% | 71 | 92.21% | 59 | 73.75% | 0.004 |
| | Present | 7 | 9.72% | 33 | 19.19% | 6 | 7.79% | 21 | 26.25% | |
| | Absent | 61 | 84.72% | 120 | 69.77% | 61 | 79.22% | 44 | 55.00% | <0.001 |
| Tumor budding | Low | 11 | 15.28% | 37 | 21.51% | 14 | 18.18% | 27 | 33.75% | |
| | High | 0 | 0.00% | 15 | 8.72% | 2 | 2.60% | 9 | 11.25% | |
| TSP | Low | 69 | 95.83% | 138 | 80.23% | 56 | 72.73% | 50 | 62.50% | <0.001 |
| | High | 3 | 4.17% | 34 | 19.77% | 21 | 27.27% | 30 | 37.50% | |
| KM grade | Low | 38 | 52.78% | 114 | 66.28% | 47 | 61.04% | 51 | 63.75% | 0.257 |
| | High | 34 | 47.22% | 58 | 33.72% | 30 | 38.96% | 29 | 36.25% | |
| | GMS 0 | 34 | 47.22% | 58 | 33.72% | 30 | 38.96% | 29 | 36.25% | <0.001 |
| GMS | GMS1 | 35 | 48.61% | 83 | 48.26% | 29 | 37.66% | 26 | 32.50% | |
| | GMS2 | 3 | 4.17% | 31 | 18.02% | 18 | 23.38% | 25 | 31.25% | |
| | Low | 23 | 31.94% | 99 | 57.89% | 46 | 59.74% | 50 | 63.29% | 0.001 |
| Immunoscore | Intermediate | 15 | 20.83% | 30 | 17.54% | 11 | 14.29% | 15 | 18.99% | |
| | High | 34 | 47.22% | 42 | 24.56% | 20 | 25.97% | 14 | 17.72% | |
| | MSS/MSI-low | 17 | 23.61% | 172 | 100.00% | 74 | 96.10% | 80 | 100.00% | <0.001 |
| MSI status | MSI-High | 55 | 76.39% | 0 | 0.00% | 3 | 3.90% | 0 | 0.00% | |

TSP: Tumor stroma percentage, KM grade: Klintrap-Makinen grade, GMS: Glasgow microenvironment score, MSS: Microsatellite stability, MSI: Microsatellite instability

Predicted NMF-based group of validation cohort using the IHC classifier also showed similar clinicopathologic characteristics of those of the training cohort. Among 401 cases, 21.7% was classified as group1 (87 cases), 23.9% as group2 (96 cases), 14.2% as group3 (57 cases), and 40.1% as group4 (161 cases).

Group 1 showed mixed MSI feature, mucinous carcinoma, exophytic growth pattern similar to those in cohort 1. MSI-High, right sided tumor, large tumor size, high proportion of poorly differentiated features, expanding growth pattern, and high KM grade were found in group 2 as expected. In group 3, tumors were located in left side dominantly and rarely produced extracellular mucin. High TSP and GMS2 were notable. In group 4, most of the tumors were located on left side. A smaller size, rare extracellular mucin formation, and relatively high TSP were also found.

Histologic features were identified and showed a similar pattern with previous molecular subtypes (Figure 8). Besides the complex tubular pattern, in CMS1, the solid feature was characteristic. Papillary and desmoplastic features were observed in CMS2. In CMS 3, papillary and serrated features were commonly found, while desmoplastic features were observed in CMS 4 next to the complex tubular feature.

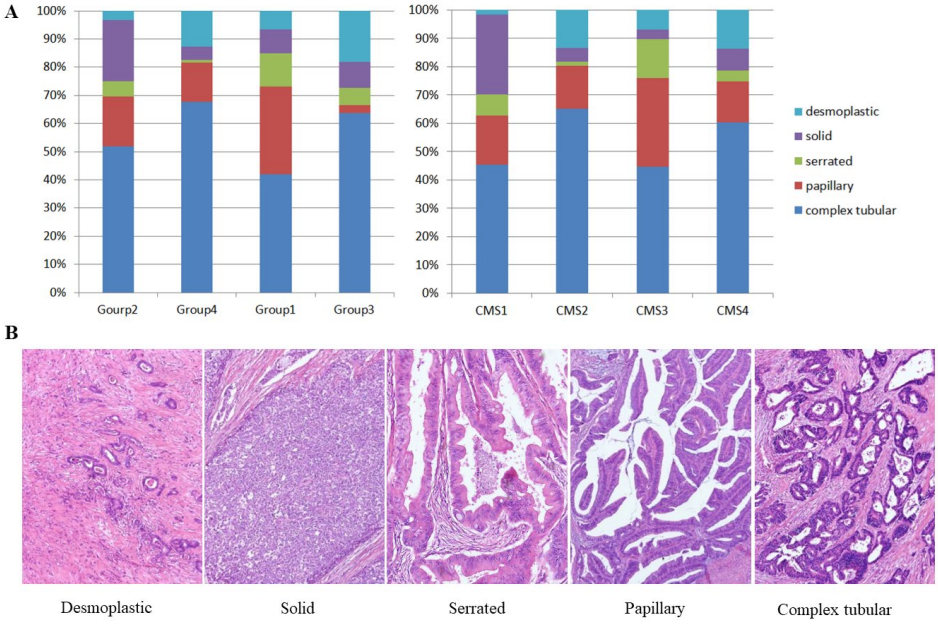

**Figure 8. Histologic features according to the predicted subtypes** (A) Major histologic features of each subtypes according to the NMF based classification and CMS classification (B) Representative image of five histologic features; desmoplastic, solid, serrated, papillary, and complex tubular pattern.

### 9. Correlation between NMF-based groups and CMSs subtyped by IHC classifier

When I compared CMSs and NMF-based groups in cohort 1, I found that 66.6% of group 2 was classified into CMS 1, 79.5% of group 4 into CMS 2, 75% of group 1 into CMS 3, and 100% of group 3 into CMS 4. I analyzed whether there were similar correlations between CMSs and NMF-based groups classified by IHC in cohort 2 (Table 9). Among the 401 cases of cohort 2, I found that group 2 was predominantly correlated with CMS 1 (55.2%), group 4 with CMS 2 (90.1%), group 1 with CMS 3 (57.5%), and group 3 with CMS 4 (77.2%), the same pattern as that observed in cohort 1.

**Table 9. Correlation between NMF based groups and CMS subtypes of cohort 2**

| | | Predicted NMF | | | | Total |
|---|---|---|---|---|---|---|
| | | Group 2 | Group 4 | Group 1 | Group 3 | |
| Predicted CMS | CMS1 | 53 (55.2%) | 0 (0%) | 19 (21.8%) | 0 (0%) | 72 |
| | CMS2 | 12(12.5%) | 145 (90.1%) | 11 (12.6%) | 4 (7.0%) | 172 |
| | CMS3 | 18 (18.8%) | 0 (0%) | 50 (57.5%) | 9 (15.8%) | 77 |
| | CMS4 | 13 (13.5%) | 16 (9.9%) | 7 (8.0%) | 44 (77.2%) | 80 |
| | Total | 96 | 161 | 87 | 57 | 401 |

**10. Patients survival analysis**

The mean follow-up time of cohort 1 was 105.85 months (ranging from 15 to 159 months). During follow-up, 13 patients (12.9%) relapsed, and eight (7.9%) died from colon cancer-related causes. The mean follow-up time of cohort 2 was 83.58 months (ranging from 1 to 110 months), with relapse in 46 patients (11.5%) and death in 76 patients (19.0%).

I compared the survival analysis according to the molecular subtypes and predicted subtypes by IHC classifier in cohort 1, which consists of stage III CRCs with FOLFOX therapy (Figure 9). When I compared prognosis between molecular subtype and predicted CMS, a similar tendency was found. For both molecular subtype and predicted subtype, CMS1 showed relatively good disease-free survival compared to CMS 3 and CMS 4. Comparison between NMF-based groups classified by molecular assay and by IHC classifier also revealed similar worse overall survival of group 1.

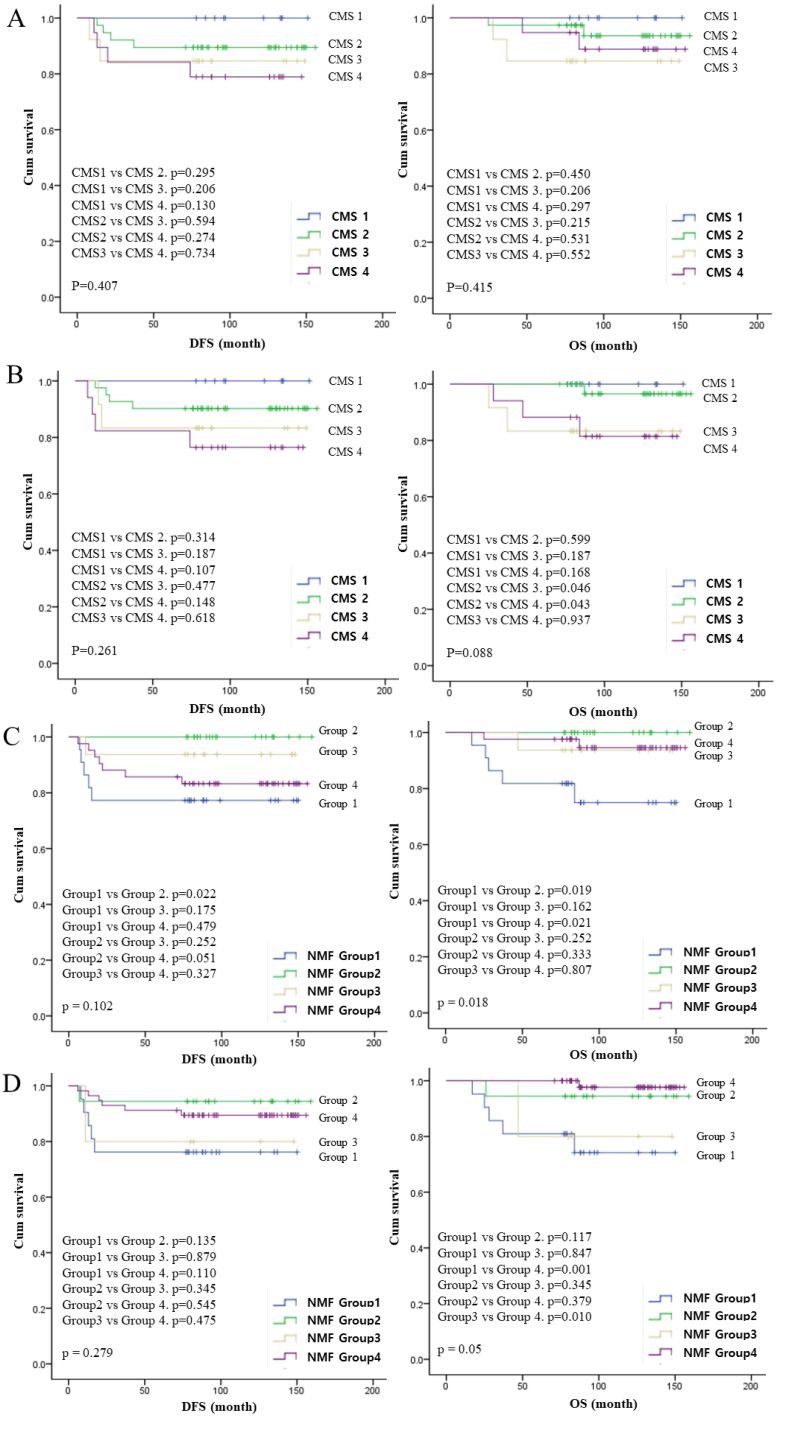

**Figure 9. Comparison of survival analysis of molecular subtypes classified by transcriptome analysis and IHC classifier in cohort 1** (A) Survival analysis of CMS classified by mRNA expression. (n=80) (B) Survival analysis of the predicted CMS by IHC. (n=80) (C) Survival analysis of NMF-based group classified by mRNA expression. (n=101) (D) Survival analysis of NMF-based group classified IHC classifier. (n=101)

I analyzed the survival of the validation cohort, which comprised CRCs ranging from stage I to IV. CMS4 showed worse DFS than CMS1, CMS2, and CMS3 ($P$ = 0.004, $P$ = 0.040, and $P$ = 0.001, respectively, figure 10A). CMS4 showed a tendency toward worse OS than CMS1. NMF-based group 3 demonstrated statistically significantly worse DFS, compared to group 1, group 2, and group 4 ($P$ = 0.001, $P$ = 0.001, and $P$ = 0.012, respectively, Figure 10B). Group 3 showed a significantly worse OS compared to group 2 (P=0.010).

I then analyzed the specific survival related stage III CRCs with FOLFOX adjuvant chemotherapy. There were 165 cases of stage III CRCs treated with FOLFOX adjuvant chemotherapy in the total cohort. Kaplan-Meier curves revealed that CMS 3 and CMS 4 showed worse prognosis in the total cohort (Figure 11).

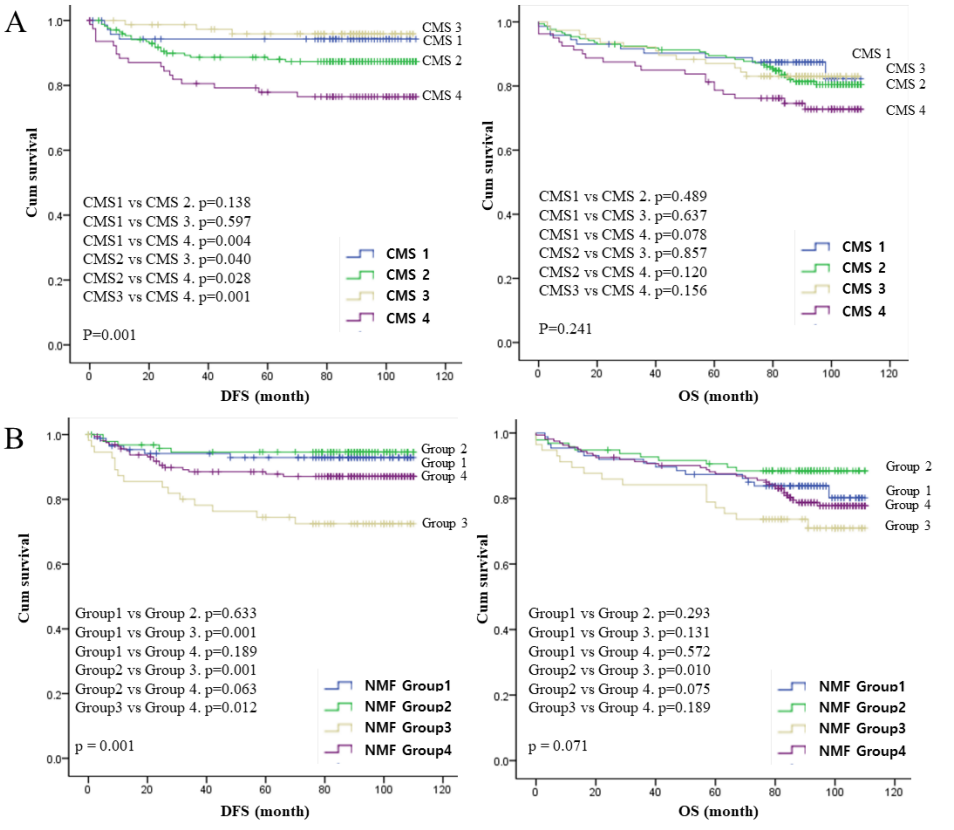


**Figure 10. Survival analysis of the predicted subtypes of the validation cohort**

(A) Survival analysis of the predicted CMS of the validation cohort. (B) Survival analysis of the predicted NMF-based group of the validation cohort.

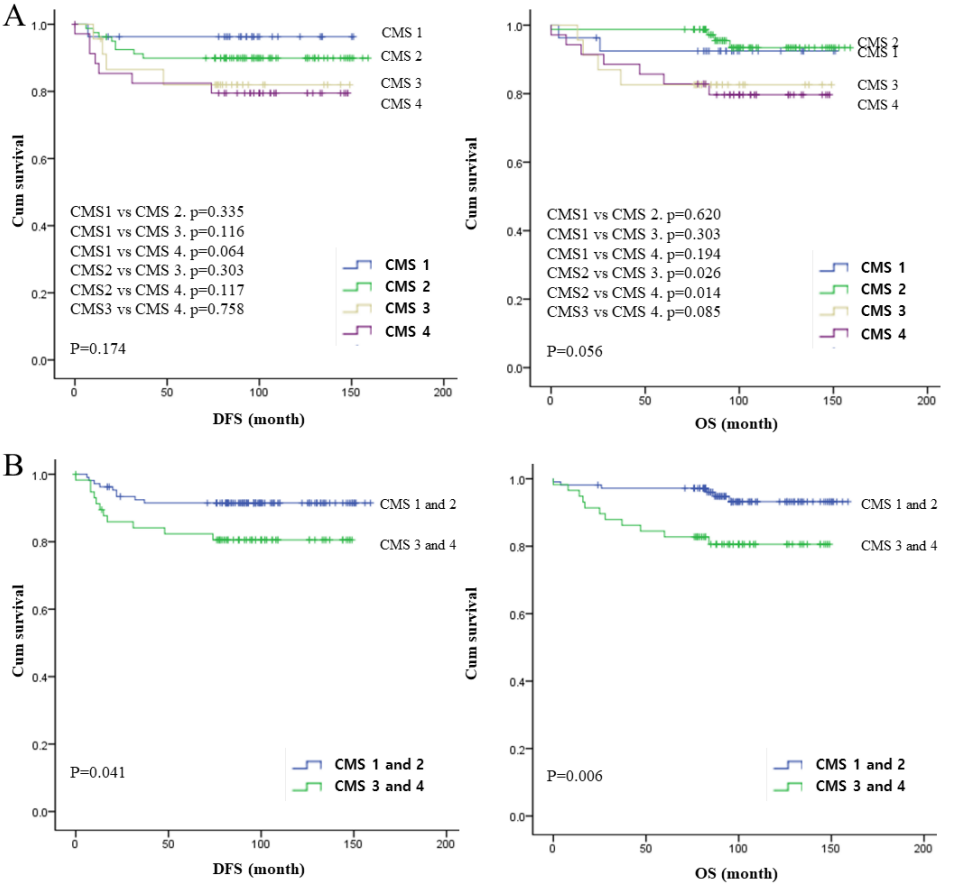


**Figure 11. Survival analysis of the predicted CMS of stage III CRCs with FOLFOX adjuvant therapy** (A) Survival analysis of the predicted CMS stage III CRCs with FOLFOX adjuvant therapy (n=165). (B) Survival analysis of the stage III CRCs with FOLFOX adjuvant therapy by CMS divided into 2 tiers (CMS 1 and 2 vs CMS 3 and 4) (n=165).

In univariate Cox-proportional hazards models for OS (Table 10), old age, increased pre-operative CEA level, non-exophytic gross type, large size, frequent tumor budding, high TSP, low immunoscore, GMS2, CMS4, and NMF group 3 were associated with a worse prognosis. Among these factors, old age, increased pre-operative CEA level, non-exophytic gross type and high TSP were independent worse prognostic factors in multivariate analysis. In univariate Cox-proportional hazards models for DFS (Table 11), MSS, increased pre-operative CEA level, non-exophytic gross type, large size, frequent tumor budding, high TSP, low immunoscore, low KM grade, GMS2, high stage, CMS4, and NMF group 3 were associated with a worse prognosis. Among these factors, CMS4, MSS, increased pre-operative CEA level, large size low immunoscore, and high stage were an independent worse prognostic factor in multivariate analysis.

**Table 10. Univariate and multivariate Cox-proportional hazards models for OS**

| | | Univariate | | | Multivariate | | |
|---|---|---|---|---|---|---|---|
| **Variable** | **Category** | **HR** | **95% CI** | **p-value** | **HR** | **95% CI** | **p-value** |
| **Age, years** | **Continuous variable** | **1.041** | **1.020-1.062** | **<0.001** | **1.036** | **1.015-1.057** | **0.001** |
| MSI | MSI-H vs. MSS(Ref.) | 0.772 | 0.353-1.690 | 0.517 | | | |
| **PreOP CEA** | **>5ng/ml vs. ≤5ng/ml(Ref.)** | **2.112** | **1.364-3.268** | **<0.001** | **1.777** | **1.130-2.794** | **0.013** |
| **Gross type** | **non-exophytic vs. exophytic(Ref.)** | **2.238** | **1.445-3.467** | **<0.001** | **2.152** | **1.366-3.389** | **0.001** |
| **Size** | **Continuous variable** | **1.111** | **1.011-1.220** | **0.029** | | | |
| **Tumor budding** | **intermediate vs. low(Ref.)** | **0.567** | **0.332-0.966** | **0.037** | | | |
| | **high vs. low(Ref.)** | **0.546** | **0.268-1.115** | **0.097** | | | |
| **TSP** | **high vs. low(Ref.)** | **2.914** | **1.825-4.653** | **<0.001** | **2.019** | **1.231-3.311** | **0.005** |
| **Immunoscore** | **intermediate vs. high(Ref.)** | **1.333** | **0.618-20877** | **0.463** | | | |
| | **low vs. high(Ref.)** | **2.228** | **1.220-4.070** | **0.009** | | | |
| **KM grade** | **high(G3-4) vs. low (G1-2)(Ref.)** | **0.504** | **0.316-0.805** | **0.004** | | | |
| **GMS** | **GMS1 vs. GMS0(Ref.)** | **1.212** | **0.702-2.093** | **0.491** | | | |
| | **GMS2 vs. GMS0(Ref.)** | **2.637** | **1.527-4.554** | **0.001** | | | |
| | StageIII/IV vs stage I/II (Ref.) | 1.371 | 0.890-2.113 | 0.152 | | | |
| **CMS** | **CMS1 vs. CMS4(Ref.)** | **0.508** | **0.771-4.064** | **0.603** | | | |
| | **CMS2 vs. CMS4(Ref.)** | **0.563** | **0.265-2.629** | **0.032** | | | |
| | **CMS3 vs. CMS4(Ref.)** | **0.708** | **1.101-6.504** | **0.285** | | | |

| | | | | |
|---|---|---|---|---|
| **NMF** | **NMF1 vs. NMF4(Ref.)** | **1.217** | **0.702-2.108** | **0.484** |
| | **NMF2 vs. NMF4(Ref.)** | **0.667** | **0.346-1.285** | **0.226** |
| | **NMF3 vs. NMF4(Ref.)** | **1.922** | **1.076-3.432** | **0.027** |

**Table 11. Univariate and multivariate Cox-proportional hazards models for DFS**

| | | Univariate | | | Multivariate | | |
|---|---|---|---|---|---|---|---|
| **Variable** | **Category** | **HR** | **95% CI** | **p-value** | **HR** | **95% CI** | **p-value** |
| Age, years | Continuous variable | 1.011 | 0.988-1.034 | 0.35 | | | |
| **MSI** | **MSI-H vs. MSS(Ref.)** | **0.109** | **0.015-0.787** | **0.028** | **0.096** | **0.011-0.880** | **0.038** |
| **PreOP CEA** | **>5ng/ml vs. ≤5ng/ml(Ref.)** | **3.015** | **1.806-5.035** | **<0.001** | **2.01** | **1.179-3.428** | **0.010** |
| **Gross type** | **non-exophytic vs. exophytic(Ref.)** | **2.741** | **1.642-4.576** | **<0.001** | | | |
| Size | Continuous variable | **1.113** | **1.002-1.235** | **0.045** | **1.185** | **1.044-1.346** | **0.009** |
| **Tumor budding** | **intermediate vs. low(Ref.)** | **0.926** | **0.493-1.740** | **0.811** | | | |
| | **high vs. low(Ref.)** | **2.397** | **1.275-4.506** | **0.007** | | | |
| **TSP** | **high vs. low(Ref.)** | **3.239** | **1.944-5.399** | **<0.001** | | | |
| **Immunoscore** | **intermediate vs. high(Ref.)** | **1.613** | **0.492-5.284** | **0.43** | | | |
| | **low vs. high(Ref.)** | **4.986** | **1.983-12.539** | **0.001** | **3.151** | **1.241-8.000** | **0.016** |
| **KM grade** | **high(G3-4) vs. low (G1-2)(Ref.)** | **0.483** | **0.275-0.849** | **0.011** | | | |
| **GMS** | **GMS1 vs. GMS0(Ref.)** | **1.516** | **0.746-3.082** | **0.25** | | | |
| | **GMS2 vs. GMS0(Ref.)** | **4.149** | **2.093-8.226** | **<0.001** | | | |
| **Stage** | **StageIII/IV vs stage I/II (Ref.)** | **2.891** | **1.628-5.132** | **<0.001** | **2.401** | **1.275-4.523** | **0.007** |
| **CMS** | **CMS1 vs. CMS4(Ref.)** | **0.242** | **0.092-0.640** | **0.004** | **0.937** | **0.311-2.827** | **0.908** |
| | **CMS2 vs. CMS4(Ref.)** | **0.480** | **0.272-0.847** | **0.011** | **0.517** | **0.277-0.964** | **0.038** |
| | **CMS3 vs. CMS4(Ref.)** | **0.265** | **0.107-0.653** | **0.004** | **0.314** | **0.122-0.804** | **0.016** |
| **NMF** | **NMF1 vs. NMF4(Ref.)** | **0.866** | **0.428-1.752** | **0.688** | | | |

| | | | |
|---|---|---|---|
| **NMF2 vs. NMF4(Ref.)** | **0.433** | **0.178-1.053** | **0.065** |
| **NMF3 vs. NMF4(Ref.)** | **2.389** | **1.281-4.453** | **0.006** |

**11. Differentially predicted subtype at the tumor center and invasion margin**

The IHC results were interpreted in the tumor center, tumor invasion margin and metastatic lymph nodes. Tumor cells in the invasion margin were considered as tumor clusters within less than 2 mm from the boundary between normal and cancer cells. Some cases showed different IHC expression patterns at the tumor center and tumor invasion margin. There were 408 cases available to evaluate CMS at both tumor center and invasion margin. Within the 86 cases classified as CMS1 at the tumor center, one case changed into CMS2, two cases into CMS3, and 5 cases into CMS4, at the invasion margin. CMS2 at the tumor center was observed in 184 cases and 4 of these changed into CMS4 at the invasion margin. The number of cases classified as CMS3 at the center was 66, and 12 of these changed into CMS2 and three into CMS1 at the invasion margin. In 72 cases of CMS4, six cases were changed into CMS2 (Figure 12).

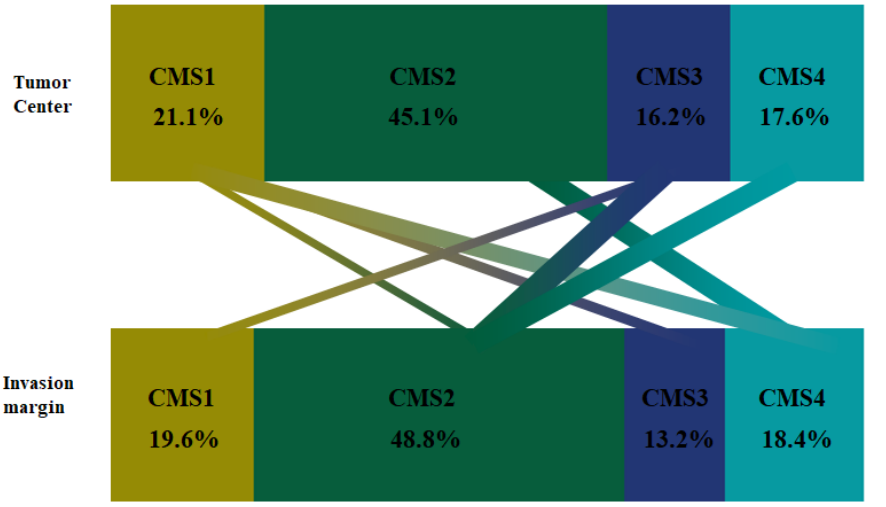


**Figure 12. Differentially predicted subtypes at the tumor center and invasion margin**

Fifty-six cases were available to evaluate the subtype classification at the tumor center, invasion margin, and metastatic lesion. There were 11 cases of CMS1, 31 cases of CMS2, and 7 cases of CMS3, with 10 cases showing differentially subtyped tumor center, invasion margin and metastatic lesion (Table 12). The immunoprofile of case 1-43 is presented in Figure 13. The case was predicted as CMS 1 at the tumor center, but changed into CMS 2 at the invasion margin and metastatic lesion. SPINK4, MUC2, and MUC5AC were highly expressed at the tumor center, but their expression was not detected in the invasion margin and metastatic lesion. Low expression of CDX2 was the characteristics of the CMS1 and CMS4. The low expression of CDX2 at the tumor center changed into high expression at the invasion margin and metastatic lesion.

**Table 12. Differentially predicted CMS at the tumor center, invasion margin, and metastatic lesion**

| Case no. | Location | Predicted CMS | SPINK4 | MUC2 | MUC5AC | TFF3 | KIT | Snail | ZMYND8 | CDX2 | MSI status |
|---|---|---|---|---|---|---|---|---|---|---|---|
| 1-57 | Tumor center | CMS1 | | ■ | | | | ■ | | ■ | ■ |
| | Invasion margin | CMS1 | | ■ | | | | ■ | | ■ | ■ |
| | Metastatic lesion | CMS3 | | | | ■ | | | | ■ | ■ |
| 1-7 | Tumor center | CMS1 | ■ | ■ | ■ | ■ | ■ | ■ | | | |
| | Invasion margin | CMS1 | ■ | | ■ | ■ | ■ | ■ | | | |
| | Metastatic lesion | CMS2 | | | | | | ■ | | | |
| **1-43** | **Tumor center** | **CMS1** | ■ | ■ | ■ | ■ | | | | | |
| | **Invasion margin** | **CMS2** | | | | ■ | | ■ | | ■ | |
| | **Metastatic lesion** | **CMS2** | | | | ■ | | | | ■ | |
| 1-47 | Tumor center | CMS1 | ■ | ■ | | ■ | | ■ | | | ■ |
| | Invasion margin | CMS3 | ■ | ■ | | ■ | | ■ | | ■ | ■ |
| | Metastatic lesion | CMS1 | | ■ | | ■ | | | | ■ | ■ |
| 1-83 | Tumor center | CMS1 | | | ■ | | | ■ | | | |
| | Invasion margin | CMS4 | ■ | | ■ | ■ | | ■ | | | |
| | Metastatic lesion | CMS1 | ■ | | ■ | | | | | | |
| 1-4 | Tumor center | CMS2 | | | | ■ | | | ■ | ■ | |
| | Invasion margin | CMS2 | | | | ■ | | | ■ | ■ | |
| | Metastatic lesion | CMS4 | | | ■ | ■ | | ■ | ■ | ■ | |
| 1-32 | Tumor center | CMS3 | ■ | ■ | | ■ | | | | ■ | |
| | Invasion margin | CMS2 | | | | ■ | | | | ■ | |
| | Metastatic lesion | CMS2 | | | | ■ | | | | ■ | |
| 1-94 | Tumor center | CMS3 | ■ | ■ | | ■ | | | ■ | | |
| | Invasion margin | CMS2 | ■ | | | ■ | | | ■ | ■ | |
| | Metastatic lesion | CMS2 | ■ | | | ■ | | | ■ | ■ | |
| 1-84 | Tumor center | CMS3 | ■ | ■ | | ■ | | | ■ | | |
| | Invasion margin | CMS2 | ■ | | | ■ | | | ■ | ■ | |
| | Metastatic lesion | CMS3 | ■ | ■ | | ■ | | | | ■ | |
| 1-51 | Tumor center | CMS3 | | ■ | | | | | | ■ | |
| | Invasion margin | CMS3 | | ■ | ■ | ■ | | | | ■ | |
| | Metastatic lesion | CMS1 | | ■ | ■ | | | | | ■ | |

Blank box : low expression, filled box: high expression or MSI-High for MSI status

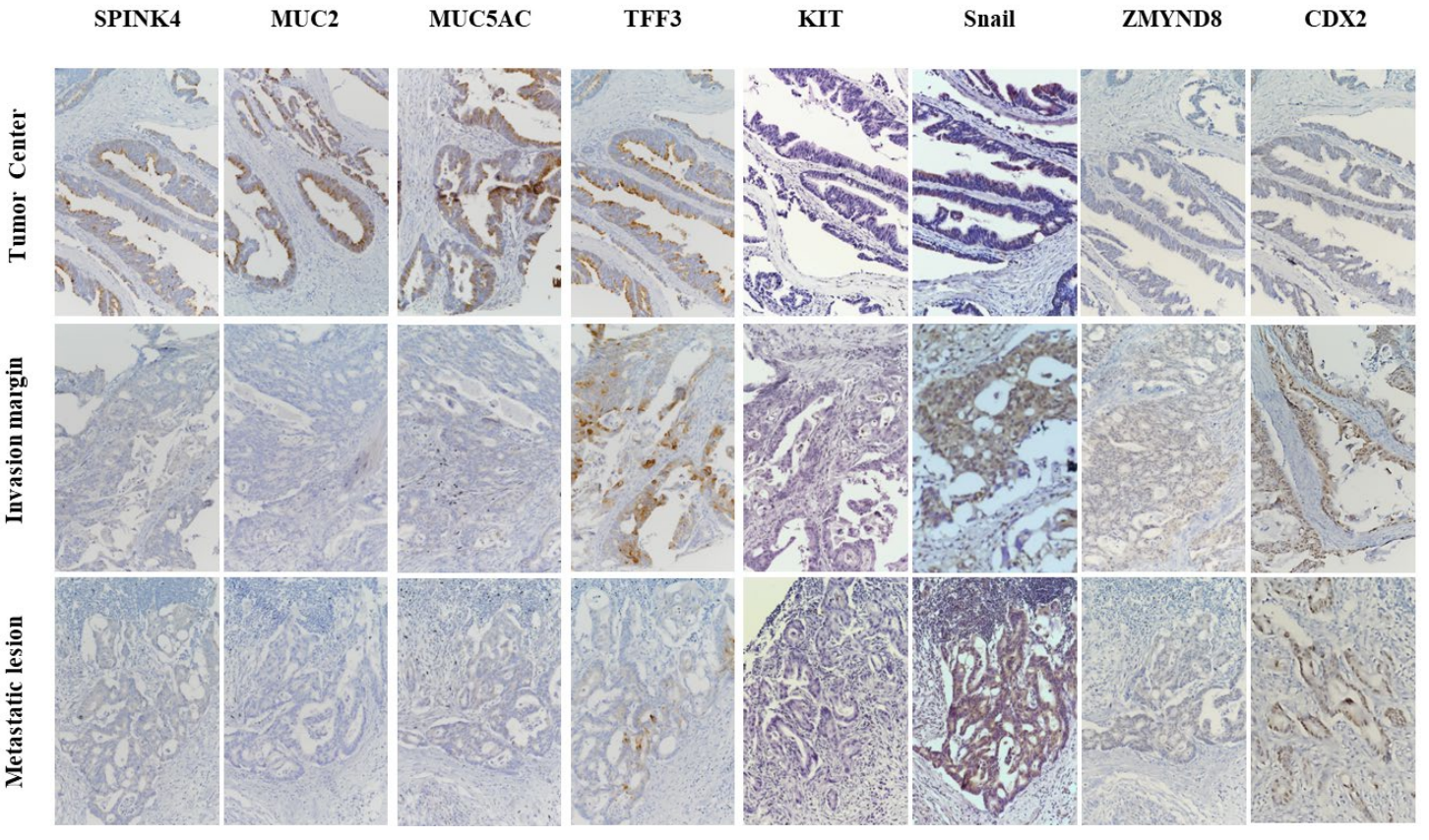


**Figure 13. The immumoprofiles of the case 1-43.**

## IV. DISCUSSION

Molecular subtyping of colorectal cancer has been improved and evolved in recent years. Until now, there has been well known simple stratification such as microsatellite instability (MSI) and chromosomal instability, providing limited prognostic information. MSI-High tumors associate with good prognosis in early stages [41], likely related to hypermutation [10,42] and cytotoxic immune cell infiltration [43]. In the metastatic setting, patients with MSI-High tumors have a poor prognosis [44], but respond well to immune checkpoint inhibition [45]. Recently, more detailed classification of primary colorectal cancer has been proposed based on intrinsic gene expression profiles resulting in the four biologically distinct consensus molecular subtypes (CMS) [11-15,17,18]. However, to reveal the molecular subtypes, the high quality genome-based transcriptome data is required from fresh tissue. It is expensive for a clinical application so far. To overcome these limitations, a method of predicting CMS using IHC or qPCR has been reported. Anne et al. divided CMSs into CMS1 (microsatellite instable), CMS2/3(epithelial-like), and CMS4 (mesenchymal) [32]. They considered MSI-High tumors as CMS1. For the rest of the cases, they used 5 IHC markers (CDX2, FRMD6, HTR2B, ZEB1 and KER) to classify epithelial (CMS2/3) or mesenchymal type (CMS4). However CMS1 consists of about 25% of MSS tumors and CMS3 is also a mixed group with MSI-High [18]. There were limitations such that CMS2 and CMS3 were considered as the same epithelial subtype. CMS1 with MSS was considered as other CMSs and CMS3 with MSI-High was categorized into CMS1 in the study. Inge et al. developed diagnostic tools using qPCR; however they focused on CMS4 (mesenchymal type) only [35]. In order to apply a practical approach in the clinical field, cost-effective and easy to applicable test is still necessary.

Here, I performed NMF consensus clustering with 1,764 DEGs in tumors compared to non-neoplastic tissues and identified four CRC molecular subtypes. When I compared our molecular subtype to CMS classification, 80 out of 101 cases were classified into one of the four groups, whereas 21 cases were not categorized and placed in the indeterminate group. I found a close correlation between group 2 and CMS1 (microsatellite instability immune), group 4 and

CMS2 (canonical), group 1 and CMS3 (metabolic, mixed MSI), and group 3 and CMS4 (mesenchymal). The characteristics of the NMF group corresponded to those of CMS. Characteristics of CMS1, such as predominant cases of MSI-High tumors, a right-sided location, high immune infiltration, and BRAF mutation detection, were observed in NMF group 2[18]. The characteristics of NMF group 4 were MSS tumors, poor immune cell infiltration, a left-sided location, and high β-catenin nuclear expression and it was similar to that of CMS2 in previous studies [18,46]. NMF-based group 1, matched with CMS3, and showed mixed MSI-High and high KRAS mutation as known as the characteristics of CMS3 [18]. High stromal infiltration (high TSP, high GMS2), MSS tumors and a left-sided location were observed in NMF-based group 3 which were matched with the mesenchymal type (CMS4) [18].

To develop the IHC classifier, I choose group-specific markers which are available to perform the immunohistochemical staining. I selected the markers that showed the same pattern in both IHC and mRNA expression with significance. Ten potential markers were selected, and used to construct the IHC classifier; SPNK4, MUC2, MUC5AC, TFF3, HTR2B, KIT, SNAI1, ZMYND8, CDX2, and MSI status. SPINK4 and MUC2, showing high expression in CMS3, are goblet cell marker [12,47]. Previous studies have suggested MUC2 as a specific marker for the goblet cell type, which corresponds to CMS3 [17,18]. Gastric foveolar mucin MUC5AC is not expressed in normal colonic mucosa. A gain of aberrant expression of MUC5AC was associated with the CpG island methylator phenotype with favorable outcome [48]. MUC5AC was highly expressed in CMS1 followed by CMS3. TFF3 is primarily produced by the colorectal mucosa [49]. TFF3 in the colorectal mucosa is predominantly expressed in the mucinous granules and involved in mucosal protection and repair in the gastrointestinal tract. High TFF3 expression in cancer cells is associated with metastasis and early recurrence and down-regulation is associated with carcinogenesis in ulcerative colitis [50,51]. In our cohort, TFF3 was decreased in CMS1 (inflammatory) and expressed normally in CMS3 (metabolic). CDX2 showed decreased expression in CMS1 and CMS4 as reported in a previous study [33]. Low expression of CDX2 in CMS4 is associated

with poor prognosis, but not in CMS1 [33,52]. HTR2B was proposed as a marker for CMS4 [32]. HTR2B induces fibrosis in liver and lung [53,54]. KIT expression is a rare event in human colorectal carcinoma[55], and showed high expression in CMS4 compared to others. Platelet-derived growth factor receptors (PDGFRs) and KIT, structurally closely related to PDGFRs, are highly co-expressed in CMS4 and inhibition of the signaling limits colon cancer invasion and the formation of distant metastases [35,56-58]. Another CMS4 marker, SNAIl, induces EMT which is predominant feature of CMS4 [59,60]. ZMYND8 was up-regulated in CMS2 and down-regulated in CMS1. It promotes tumor angiogenesis via induction of vascular endothelial growth factor-A expression [61]. ZMYND8 play a role in silencing tumor suppressor genes by recruiting CHD4 and induces early disease recurrence [62]. MSI-High is predominantly observed in CMS1. CMS3 is a mixed type with a small proportion of MSI-High.

The IHC classifier for CMS showed higher accuracy (0.812, 95% CI = 0.737 - 0.825) and lower AIC (134.771, 95% CI = 134.507 - 160.549) than that for NMF-based group (accuracy: 0.702, 95% CI = 0.643 - 0.702 and AIC: 226.576, 95% CI = 226.576 - 237.358). To establish the IHC classifiers, I input the data of 101 cases of cohort 1 for NMF-based group and 80cases for CMSs except for unclassifiable cases. Even though more information was used in classifier for NMF, accuracy was lower, and AIC was higher than the classifier for CMS. It showed that even though there exists a high similarity between NMF-based group and CMSs, CMS has more distinct characteristics and more reproducible through the IHC. The characteristics of predicted subtypes by the IHC classifier were similar to that of the molecular subtypes classified by mRNA expression. CMS1/NMF-based group 2 included a high proportion of MSI-High tumors. The characteristic of MSI-High tumors such as a right-sided location, larger size, a large proportion of mucinous carcinoma (>50% of extracellular mucin formation), and Crohn-like lymphoid reaction was frequently found. Moreover relatively low TSP, high KM grade, high proportion of GMS0, and a high immunoscore was also observed.

CMS2/NMF-based group 4 showed stable microsatellite status, left-sided features,

small tumor size, infiltrative invasion pattern, and relatively poor immune cell infiltration. CMS3 was characterized by mixed MSI-High, mucinous carcinoma (>50% of extracellular mucin formation), rare lymphovascular invasion and tumor budding. CMS4/NMF-based group 3 is well known to cause poor prognosis and increased stromal infiltration, and the predicted groups also represented high TSP and a large proportion of GMS2. The GMS, the combination score of TSP and KM grade, represent worst prognosis as it increased [40]. Moreover other poor prognostic factors such as infiltrative growth pattern, frequent lymphovascular invasion and tumor budding were significant. The prognosis of CRCs with stage I to IV showed the worst prognosis in CMS4 (DFS: P = 0.001, OS: P = 0.241) which was similar to the previous data [18,19]. When I evaluated the prognosis of the stage III CRCs treated by FOLFOX regimen, the disease-free survival curve for the CMS showed a worst outcome in CMS3 and CMS4. CMS 4 is well known as poor prognostic subtype regardless of chemotherapy in previous studies [18,19]. From the previous study of Song et al, CMS2 showed favorable prognosis in Stage II/III CRC treated using oxaliplatin plus fluorouracil-leucovorin (FOLFOX) than fluorouracil plus leucovorin, and CMS4 revealed poor prognosis regardless of the chemotherapy regimen[19]. Interestingly, CMS3 did not favor chemotherapy with oxaliplatin (HR 1.17, 95% CI = 0.54 - 2.53) [19]. KRAS mutation is frequently found in CMS3 than in other CMSs. KRAS mutation is a poor predictive marker of poor response for anti-EGFR therapy efficacy in metastatic CRC [63], while the evidence of a prognostic impact is more ambiguous. Studies on stages I–III disease have shown inconsistent associations with survival [64-66] but a recent study indicated a negative prognostic impact after relapse[67]. In association with adjuvant FOLFOX chemotherapy, some studies elucidated that KRAS mutation did not affect the impact on PFS or OS [65,68]. However, when stratified according to the primary tumor site and MSI status, KRAS mutation is suggested to have distinct negative prognostic effect [69,70]. In our data, patients with KRAS mutation had worse OS and DFS than patients with wild type KRAS in stage III CRCs with FOLFOX chemotherapy. The poor prognosis of CMS3 and CMS 4 stage III CRCs with FOLFOX chemotherapy can be considered due to its own worse prognosis

for CMS4 and poor response to FOLFOX regimen for CMS3. However, a detailed comprehensive study is still required.

Specific characters of molecular subtype may provide a rationale for the assignment of patients to different treatment regimens, such as oxaliplatin-based chemotherapy for patients or addition of bevacizumab to first-line capecitabine-based chemotherapy for CMS2[71] and immune checkpoint inhibitors for CMS1.

For CMS3, bevacizumab to first-line capecitabine-based chemotherapy can be considered [71]. CMS4 tumors are characterized by high expression of genes reflecting epithelial-to-mesenchymal transition (EMT), transforming growth factor (TGF)-β signaling, and matrix remodeling and have high stromal cell content. Increased TGF-β plays a crucial rule in EMT, angiogenesis, and immune suppression [72-75]. TGF-β induces angiogenesis through vascular endothelial growth factor (VEGF) mediated apoptosis [74]. VEGF regulates not only angiogenesis but also the intratumoral immune response by inhibiting the migration of T cells to the intratumoral lesion and inducing PD-1 expression and other inhibitory checkpoints resulting in CD8 T cell exhaustion [76]. VEGF and/or TGF-β silencing markedly improved the efficacy of anti–PD-1/anti–CTLA-4 treatment [77]. Therefore, combined TGF pathway inhibition/angiogenesis blockade and immune checkpoint inhibition is expected to have a synergic effect on CMS4.

De Smedt et al. performed the microdissection and processed RNA-sequencing to tumor bulk and budding, and revealed that seven tumor bulk were classified to CMS2, whereas the five tumor budding closely matched the CMS4 subtype [78]. For one sample, the tumor budding signature was classified as CMS1. In our study, among 408 cases, 33 cases (8.1%) showed subtype discrepancy between tumor center and margin. Changes into CMS2 at the invasion margin were most frequently observed (19/33). The subtype discrepancy into CMS 4 was followed (9/33). Moreover, of the 56 cases analyzed, ten cases showed subtype discrepancy in the tumor center, invasion margin, and metastatic lesion. Interestingly, there were 3 cases showing the same CMS subtype in the tumor center and metastatic lesion but not in invasion margin. This finding shows that tumor composed of heterogeneous cell types, and they metastasize regardless of their type and location

(center or invasion margin). Claudio et al. observed that, among the eleven pretreatment biopsies assigned preferentially to the CMS2, eight cases were classified to the CMS4 in the post-treatment specimens. Notably, in two of these cases, in which the patients underwent complete response, the post-treatment surgical samples were histologically described as fibrous scars [79]. This finding can be considered as both increase fibroblasts in the post-treatment specimen or subtype changes. There has been a concern that the molecular signature of CMS4 might have originated from the large proportion of fibroblast in the increased extracellular matrix due to the disappearance of only CMS4 signature when the PDX model was studied using variable CMSs [31,79,80]. To resolve the problem, I conducted microdissection to increase tumor proportion of the tissue to 70%. As a result, our data represent the tumor-specific gene expression with relatively low contents of peritumoral stromal cells. Furthermore, compared to the transcriptome-based subtyping, IHC classifier reduced the interference of the fibroblast as it detects the protein expression in the tumor only.

Using markers for the molecular subtype, I established the IHC classifier and the characteristics of predicted subtypes were similar to those of the subtypes classified by gene expression data. Even though I understand the limitations of the study, such as consistency of interpretation and stain quality, there are benefits as well, such as cost effectiveness and easy applicability. Moreover, IHC classifier will reduce biased information by the stromal contents than the molecular test.

## V. CONCLUSION

In conclusion, I an established IHC subtype classifier, which predicts the molecular subtypes of CRCs. Predicted subtype represented the clinicopathologic characteristics of molecular subtypes with benefits such as cost-effectiveness and easy applicability. The IHC classifier also reduced biased information by the stromal contents rather than the molecular test. Using the IHC classifier, I found that CMS 3 and CMS4 showed poor prognosis after FOLFOX chemotherapy. My study proposes a practical IHC classifier to identify molecular subtypes and to guide subtype specific therapeutic approach in CRCs.

## REFERENCES

1. Siegel RL, Miller KD, Jemal A. Cancer statistics, 2018. CA Cancer J Clin 2018;68:7-30.
2. Miller KD, Siegel RL, Lin CC, Mariotto AB, Kramer JL, Rowland JH, et al. Cancer treatment and survivorship statistics, 2016. CA Cancer J Clin 2016;66:271-89.
3. Andre T, Boni C, Mounedji-Boudiaf L, Navarro M, Tabernero J, Hickish T, et al. Oxaliplatin, fluorouracil, and leucovorin as adjuvant treatment for colon cancer. N Engl J Med 2004;350:2343-51.
4. Benson AB, 3rd. Adjuvant chemotherapy of stage III colon cancer. Semin Oncol 2005;32:S74-7.
5. Stefansson M, Nygren P. Oxaliplatin added to fluoropyrimidine for adjuvant treatment of colorectal cancer is associated with long-term impairment of peripheral nerve sensory function and quality of life. Acta Oncol 2016;55:1227-35.
6. Des Guetz G, Schischmanoff O, Nicolas P, Perret GY, Morere JF, Uzzan B. Does microsatellite instability predict the efficacy of adjuvant chemotherapy in colorectal cancer? A systematic review with meta-analysis. Eur J Cancer 2009;45:1890-6.
7. Sinicrope FA, Sargent DJ. Clinical implications of microsatellite instability in sporadic colon cancers. Curr Opin Oncol 2009;21:369-73.
8. De Roock W, Claes B, Bernasconi D, De Schutter J, Biesmans B, Fountzilas G, et al. Effects of KRAS, BRAF, NRAS, and PIK3CA mutations on the efficacy of cetuximab plus chemotherapy in chemotherapy-refractory metastatic colorectal cancer: a retrospective consortium analysis. Lancet Oncol 2010;11:753-62.
9. Lievre A, Bachet JB, Le Corre D, Boige V, Landi B, Emile JF, et al. KRAS mutation status is predictive of response to cetuximab therapy in colorectal cancer. Cancer Res 2006;66:3992-5.
10. Comprehensive molecular characterization of human colon and rectal cancer. Nature 2012;487:330-7.
11. Roepman P, Schlicker A, Tabernero J, Majewski I, Tian S, Moreno V, et al. Colorectal cancer intrinsic subtypes predict chemotherapy benefit, deficient mismatch repair and epithelial-to-mesenchymal transition. Int J Cancer 2014;134:552-62.
12. Budinska E, Popovici V, Tejpar S, D'Ario G, Lapique N, Sikora KO, et al. Gene expression patterns unveil a new level of molecular heterogeneity in colorectal cancer. J Pathol 2013;231:63-76.
13. De Sousa EMF, Wang X, Jansen M, Fessler E, Trinh A, de Rooij LP, et al. Poor-prognosis colon cancer is defined by a molecularly distinct subtype and develops from serrated precursor lesions. Nat Med

2013;19:614-8.
14. Marisa L, de Reynies A, Duval A, Selves J, Gaub MP, Vescovo L, et al. Gene expression classification of colon cancer into molecular subtypes: characterization, validation, and prognostic value. PLoS Med 2013;10:e1001453.
15. Schlicker A, Beran G, Chresta CM, McWalter G, Pritchard A, Weston S, et al. Subtypes of primary colorectal tumors correlate with response to targeted treatment in colorectal cell lines. BMC Med Genomics 2012;5:66.
16. Perez-Villamil B, Romera-Lopez A, Hernandez-Prieto S, Lopez-Campos G, Calles A, Lopez-Asenjo JA, et al. Colon cancer molecular subtypes identified by expression profiling and associated to stroma, mucinous type and different clinical behavior. BMC Cancer 2012;12:260.
17. Sadanandam A, Lyssiotis CA, Homicsko K, Collisson EA, Gibb WJ, Wullschleger S, et al. A colorectal cancer classification system that associates cellular phenotype and responses to therapy. Nat Med 2013;19:619-25.
18. Guinney J, Dienstmann R, Wang X, de Reynies A, Schlicker A, Soneson C, et al. The consensus molecular subtypes of colorectal cancer. Nat Med 2015;21:1350-6.
19. Song N, Pogue-Geile KL, Gavin PG, Yothers G, Kim SR, Johnson NL, et al. Clinical Outcome From Oxaliplatin Treatment in Stage II/III Colon Cancer According to Intrinsic Subtypes: Secondary Analysis of NSABP C-07/NRG Oncology Randomized Clinical Trial. JAMA Oncol 2016;2:1162-9.
20. Bolstad BM, Irizarry RA, Astrand M, Speed TP. A comparison of normalization methods for high density oligonucleotide array data based on variance and bias. Bioinformatics 2003;19:185-93.
21. Lee HJ, Suk JE, Patrick C, Bae EJ, Cho JH, Rho S, et al. Direct transfer of alpha-synuclein from neuron to astroglia causes inflammatory responses in synucleinopathies. J Biol Chem 2010;285:9262-72.
22. Hwang D, Rust AG, Ramsey S, Smith JJ, Leslie DM, Weston AD, et al. A data integration methodology for systems biology. Proc Natl Acad Sci U S A 2005;102:17296-301.
23. Tibshirani R, Hastie T, Narasimhan B, Chu G. Diagnosis of multiple cancer types by shrunken centroids of gene expression. Proc Natl Acad Sci U S A 2002;99:6567-72.
24. Huang da W, Sherman BT, Lempicki RA. Systematic and integrative analysis of large gene lists using DAVID bioinformatics resources. Nat Protoc 2009;4:44-57.
25. Brunet JP, Tamayo P, Golub TR, Mesirov JP. Metagenes and molecular pattern discovery using matrix factorization. Proc Natl Acad Sci U S A

2004;101:4164-9.
26. Gao Y, Church G. Improving molecular cancer class discovery through sparse non-negative matrix factorization. Bioinformatics 2005;21:3970-5.
27. Kim H, Park H. Sparse non-negative matrix factorizations via alternating non-negativity-constrained least squares for microarray data analysis. Bioinformatics 2007;23:1495-502.
28. Gaujoux R, Seoighe C. A flexible R package for nonnegative matrix factorization. BMC Bioinformatics 2010;11:367.
29. Langfelder P, Horvath S. WGCNA: an R package for weighted correlation network analysis. BMC Bioinformatics 2008;9:559.
30. Chen D, Qi W, Zhang P, Zhang Y, Liu Y, Guan H, et al. Investigation of BRAF V600E detection approaches in papillary thyroid carcinoma. Pathol Res Pract 2018;214:303-7.
31. Isella C, Brundu F, Bellomo SE, Galimi F, Zanella E, Porporato R, et al. Selective analysis of cancer-cell intrinsic transcriptional traits defines novel clinically relevant subtypes of colorectal cancer. Nat Commun 2017;8:15107.
32. Trinh A, Trumpi K, De Sousa EMF, Wang X, de Jong JH, Fessler E, et al. Practical and Robust Identification of Molecular Subtypes in Colorectal Cancer by Immunohistochemistry. Clin Cancer Res 2017;23:387-98.
33. Pilati C, Taieb J, Balogoun R, Marisa L, de Reynies A, Laurent-Puig P. CDX2 prognostic value in stage II/III resected colon cancer is related to CMS classification. Ann Oncol 2017;28:1032-5.
34. Wang WH, Xie TY, Xie GL, Ren ZL, Li JM. An Integrated Approach for Identifying Molecular Subtypes in Human Colon Cancer Using Gene Expression Data. Genes (Basel) 2018;9.
35. Ubink I, Elias SG, Moelans CB, Lacle MM, van Grevenstein WMU, van Diest PJ, et al. A Novel Diagnostic Tool for Selecting Patients With Mesenchymal-Type Colon Cancer Reveals Intratumor Subtype Heterogeneity. J Natl Cancer Inst 2017;109.
36. Taube JM, Galon J, Sholl LM, Rodig SJ, Cottrell TR, Giraldo NA, et al. Implications of the tumor immune microenvironment for staging and therapeutics. Mod Pathol 2018;31:214-34.
37. Kwak Y, Koh J, Kim DW, Kang SB, Kim WH, Lee HS. Immunoscore encompassing CD3+ and CD8+ T cell densities in distant metastasis is a robust prognostic marker for advanced colorectal cancer. Oncotarget 2016;7:81778-90.
38. Huijbers A, Tollenaar RA, v Pelt GW, Zeestraten EC, Dutton S, McConkey CC, et al. The proportion of tumor-stroma as a strong prognosticator for stage II and III colon cancer patients: validation in the VICTOR trial. Ann Oncol 2013;24:179-85.

39. Roxburgh CS, Salmond JM, Horgan PG, Oien KA, McMillan DC. Comparison of the prognostic value of inflammation-based pathologic and biochemical criteria in patients undergoing potentially curative resection for colorectal cancer. Ann Surg 2009;249:788-93.
40. Park JH, McMillan DC, Powell AG, Richards CH, Horgan PG, Edwards J, et al. Evaluation of a tumor microenvironment-based prognostic score in primary operable colorectal cancer. Clin Cancer Res 2015;21:882-8.
41. Popat S, Hubner R, Houlston RS. Systematic review of microsatellite instability and colorectal cancer prognosis. J Clin Oncol 2005;23:609-18.
42. Vogelstein B, Papadopoulos N, Velculescu VE, Zhou S, Diaz LA, Jr., Kinzler KW. Cancer genome landscapes. Science 2013;339:1546-58.
43. Mlecnik B, Bindea G, Angell HK, Maby P, Angelova M, Tougeron D, et al. Integrative Analyses of Colorectal Cancer Show Immunoscore Is a Stronger Predictor of Patient Survival Than Microsatellite Instability. Immunity 2016;44:698-711.
44. Kim CG, Ahn JB, Jung M, Beom SH, Kim C, Kim JH, et al. Effects of microsatellite instability on recurrence patterns and outcomes in colorectal cancers. Br J Cancer 2016;115:25-33.
45. Le DT, Uram JN, Wang H, Bartlett BR, Kemberling H, Eyring AD, et al. PD-1 Blockade in Tumors with Mismatch-Repair Deficiency. N Engl J Med 2015;372:2509-20.
46. Roelands J, Kuppen PJK, Vermeulen L, Maccalli C, Decock J, Wang E, et al. Immunogenomic Classification of Colorectal Cancer and Therapeutic Implications. Int J Mol Sci 2017;18.
47. Noah TK, Kazanjian A, Whitsett J, Shroyer NF. SAM pointed domain ETS factor (SPDEF) regulates terminal differentiation and maturation of intestinal goblet cells. Exp Cell Res 2010;316:452-65.
48. Betge J, Schneider NI, Harbaum L, Pollheimer MJ, Lindtner RA, Kornprat P, et al. MUC1, MUC2, MUC5AC, and MUC6 in colorectal cancer: expression profiles and clinical significance. Virchows Arch 2016;469:255-65.
49. Suemori S, Lynch-Devaney K, Podolsky DK. Identification and characterization of rat intestinal trefoil factor: tissue- and cell-specific member of the trefoil protein family. Proc Natl Acad Sci U S A 1991;88:11017-21.
50. Morito K, Nakamura J, Kitajima Y, Kai K, Tanaka T, Kubo H, et al. The value of trefoil factor 3 expression in predicting the longterm outcome and early recurrence of colorectal cancer. Int J Oncol 2015;46:563-8.
51. Kondo S, Araki T, Toiyama Y, Tanaka K, Kawamura M, Okugawa Y, et al. Downregulation of trefoil factor-3 expression in the rectum is associated with the development of ulcerative colitis-associated cancer.

Oncol Lett 2018;16:3658-64.
52. Ryan EJ, Creavin B, Khaw YL, Kelly ME, Mohan HM, Geraghty R, et al. Effects of CDX2 on prognosis and chemotherapy responsiveness in mismatch repair-deficient colorectal cancer. BJS Open 2018;2:456-63.
53. Yang Q, Yan C, Gong Z. Interaction of hepatic stellate cells with neutrophils and macrophages in the liver following oncogenic kras activation in transgenic zebrafish. Sci Rep 2018;8:8495.
54. Tu RF, Zhang XF, He ZH. [The expression of 5-HTR2BE-cadalpha-SMA in the pulmonary fibrosis in rats]. Zhongguo Ying Yong Sheng Li Xue Za Zhi 2016;32:365-9.
55. Reed J, Ouban A, Schickor FK, Muraca P, Yeatman T, Coppola D. Immunohistochemical staining for c-Kit (CD117) is a rare event in human colorectal carcinoma. Clin Colorectal Cancer 2002;2:119-22.
56. Steller EJ, Raats DA, Koster J, Rutten B, Govaert KM, Emmink BL, et al. PDGFRB promotes liver metastasis formation of mesenchymal-like colorectal tumor cells. Neoplasia 2013;15:204-17.
57. Shinagawa K, Kitadai Y, Tanaka M, Sumida T, Onoyama M, Ohnishi M, et al. Stroma-directed imatinib therapy impairs the tumor-promoting effect of bone marrow-derived mesenchymal stem cells in an orthotopic transplantation model of colon cancer. Int J Cancer 2013;132:813-23.
58. Kitadai Y, Sasaki T, Kuwai T, Nakamura T, Bucana CD, Fidler IJ. Targeting the expression of platelet-derived growth factor receptor by reactive stroma inhibits growth and metastasis of human colon carcinoma. Am J Pathol 2006;169:2054-65.
59. Pena C, Garcia JM, Larriba MJ, Barderas R, Gomez I, Herrera M, et al. SNAI1 expression in colon cancer related with CDH1 and VDR downregulation in normal adjacent tissue. Oncogene 2009;28:4375-85.
60. Kim YH, Kim G, Kwon CI, Kim JW, Park PW, Hahm KB. TWIST1 and SNAI1 as markers of poor prognosis in human colorectal cancer are associated with the expression of ALDH1 and TGF-beta1. Oncol Rep 2014;31:1380-8.
61. Kuroyanagi J, Shimada Y, Zhang B, Ariyoshi M, Umemoto N, Nishimura Y, et al. Zinc finger MYND-type containing 8 promotes tumour angiogenesis via induction of vascular endothelial growth factor-A expression. FEBS Lett 2014;588:3409-16.
62. Xia L, Huang W, Bellani M, Seidman MM, Wu K, Fan D, et al. CHD4 Has Oncogenic Functions in Initiating and Maintaining Epigenetic Suppression of Multiple Tumor Suppressor Genes. Cancer Cell 2017;31:653-68.e7.
63. Van Cutsem E, Cervantes A, Adam R, Sobrero A, Van Krieken JH, Aderka D, et al. ESMO consensus guidelines for the management of patients with metastatic colorectal cancer. Ann Oncol 2016;27:1386-422.

64. Roth AD, Tejpar S, Delorenzi M, Yan P, Fiocca R, Klingbiel D, et al. Prognostic role of KRAS and BRAF in stage II and III resected colon cancer: results of the translational study on the PETACC-3, EORTC 40993, SAKK 60-00 trial. J Clin Oncol 2010;28:466-74.
65. Deng Y, Wang L, Tan S, Kim GP, Dou R, Chen D, et al. KRAS as a predictor of poor prognosis and benefit from postoperative FOLFOX chemotherapy in patients with stage II and III colorectal cancer. Mol Oncol 2015;9:1341-7.
66. Andreyev HJ, Norman AR, Cunningham D, Oates J, Dix BR, Iacopetta BJ, et al. Kirsten ras mutations in patients with colorectal cancer: the 'RASCAL II' study. Br J Cancer 2001;85:692-6.
67. Sinicrope FA, Shi Q, Allegra CJ, Smyrk TC, Thibodeau SN, Goldberg RM, et al. Association of DNA Mismatch Repair and Mutations in BRAF and KRAS With Survival After Recurrence in Stage III Colon Cancers : A Secondary Analysis of 2 Randomized Clinical Trials. JAMA Oncol 2017;3:472-80.
68. Richman SD, Seymour MT, Chambers P, Elliott F, Daly CL, Meade AM, et al. KRAS and BRAF mutations in advanced colorectal cancer are associated with poor prognosis but do not preclude benefit from oxaliplatin or irinotecan: results from the MRC FOCUS trial. J Clin Oncol 2009;27:5931-7.
69. Blons H, Emile JF, Le Malicot K, Julie C, Zaanan A, Tabernero J, et al. Prognostic value of KRAS mutations in stage III colon cancer: post hoc analysis of the PETACC8 phase III trial dataset. Ann Oncol 2014;25:2378-85.
70. Taieb J, Le Malicot K, Shi Q, Penault-Llorca F, Bouche O, Tabernero J, et al. Prognostic Value of BRAF and KRAS Mutations in MSI and MSS Stage III Colon Cancer. J Natl Cancer Inst 2017;109.
71. Mooi JK, Wirapati P, Asher R, Lee CK, Savas P, Price TJ, et al. The prognostic impact of consensus molecular subtypes (CMS) and its predictive effects for bevacizumab benefit in metastatic colorectal cancer: molecular analysis of the AGITG MAX clinical trial. Ann Oncol 2018;29:2240-6.
72. Xu J, Lamouille S, Derynck R. TGF-beta-induced epithelial to mesenchymal transition. Cell Res 2009;19:156-72.
73. Katsuno Y, Lamouille S, Derynck R. TGF-beta signaling and epithelial-mesenchymal transition in cancer progression. Curr Opin Oncol 2013;25:76-84.
74. Ferrari G, Cook BD, Terushkin V, Pintucci G, Mignatti P. Transforming growth factor-beta 1 (TGF-beta1) induces angiogenesis through vascular endothelial growth factor (VEGF)-mediated apoptosis. J Cell Physiol 2009;219:449-58.
75. Wrzesinski SH, Wan YY, Flavell RA. Transforming growth factor-beta

and the immune response: implications for anticancer therapy. Clin Cancer Res 2007;13:5262-70.

76. Rivera LB, Bergers G. Intertwined regulation of angiogenesis and immunity by myeloid cells. Trends Immunol 2015;36:240-9.

77. Courau T, Nehar-Belaid D, Florez L, Levacher B, Vazquez T, Brimaud F, et al. TGF-beta and VEGF cooperatively control the immunotolerant tumor environment and the efficacy of cancer immunotherapies. JCI Insight 2016;1:e85974.

78. De Smedt L, Palmans S, Andel D, Govaere O, Boeckx B, Smeets D, et al. Expression profiling of budding cells in colorectal cancer reveals an EMT-like phenotype and molecular subtype switching. Br J Cancer 2017;116:58-65.

79. Isella C, Terrasi A, Bellomo SE, Petti C, Galatola G, Muratore A, et al. Stromal contribution to the colorectal cancer transcriptome. Nat Genet 2015;47:312-9.

80. Schutte M, Risch T, Abdavi-Azar N, Boehnke K, Schumacher D, Keil M, et al. Molecular dissection of colorectal cancer in pre-clinical models identifies biomarkers predicting sensitivity to EGFR inhibitors. Nat Commun 2017;8:14262.

**ABSTRACT (IN KOREAN)**

# 대장직장암의 면역조직화학염색기반 분자아형분류의 개발 : 전사체 분석과 면역조직화학염색의 상호연관성

<지도교수 김 호 근>

연세대학교 대학원 의학과

장 미

대장 직장암 환자에서 진행된 대장직장암 환자를 대상으로 수술적 제거 이후 FOLFOX 항암화학요법을 주로 시행하고 있으나 임상적인 효과는 다양하게 나타난다. 개인맞춤형 치료전략을 수행하기 위해서는 적합한 바이오마커를 발굴하여 치료반응을 예측할 수 있는 분자아형을 분류하는 것이 요구된다.

본 연구는 FOLFOX 항암화학요법을 시행한 3기 대장암을 대상으로 유전자발현 정보를 분석하여 분자아형을 분류하였으며 면역조직화학염색을 통하여 분자아형을 재연할 수 있는 알고리즘를 개발하는 것을 목적으로 하였다.

트레이닝 코호트 (101 개의 FOLFOX 항암화학요법을 시행한 3기 대장암)의 전사체 발현을 이용하여 NMF (Non-negative Matrix Factorization) 기반의 4개의 분자아형을 나누었으며 이는 기존 연구에서 제시된 콘센서스 분자아형(CMS)과 79% 의 유사성을 보이는 것으로 나타났으며 서로 관련성을 보이는 아형의 임상병리학적 특징이 유사하였다.

면역조직화학염색 분류 알고리즘을 위한 마커를 선정하기 위하여 다른 그룹들이나 정상점막보다 1.5배 이상의 발현증가를 보이는 13개의 면역화학염색이 가능한 표지자를 선별하였으며, 이에 추가로 이전 연구에서 분자아형의 마커로 제시된 19개의 표지자를 선택하였다. 면역조직화학염색의 결과를 평가하여 그룹간에 현저하게 다른 표현을

보여주는 9개의 인자를 선정했다. SNAI1, MUC2, SPINK4, KIT, CDX2, ZMYND8, TFF3, MUC5AC, 그리고 MSI status 를 마커로 사용하였을 때 콘센서스 분자아형(CMS)을 효과적으로 분류하였다 (accuracy: 0.825, 95% CI=0.737-0.825, AIC: 134.771, 95% CI = 134.507-160.549). 이들 인자에서 KIT를 HTR2B으로 변경함으로 NMF 기반 분자아형의 예측을 최적화 할 수 있었다 (accuracy: 0.702, 95% CI=0.643-0.702, AIC: 226.576, 95% CI = 226.576-237.358). 면역조직화학염색 알고리즘을 검증 코호트에 적용하여 분류된 분자아형은 기존의 분자아형의 특성을 유의하게 보였으며 CMS4의 나쁜 예후를 나타냈다. 또한 CMS3와 CMS4가 FOLFOX 화학요법에 나쁜 예후를 보이는 것을 관찰하였다. 종양의 중심부와 주변 침윤부의 분자아형을 비교하였을 때 406 개의 케이스에서 약 8.1% 가 중심부와 주변 침윤부의 분자아형이 다르게 분류되었다.

이러한 면역조직화학염색 알고리즘을 이용한 분자아형분류를 통하여 효율적이고 낮은 비용으로 분자아형을 예측할 수 있으며, 치료반응을 예측하는데 도움을 얻을 수 있고, 종양세포자체의 단백질 발현으로 분류하기 때문에 기존의 전사체 발현을 통한 분류에서 섬유아세포 및 기질에 의해 영향을 받던 단점을 보완할 수 있을 것으로 판단된다.

핵심되는 말: 대장직장암, 전사체 기반 분자 아형 분류, 분자 아형, 콘센서스 분자아형 (CMS), 면역조직화학염색 알고리즘, FOLFOX 항암화학요법

# PUBLICATION LIST

Kwon Y, Park M, Jang M, Yun S, Kim WK, Kim S, et al. Prognosis of stage III colorectal carcinomas with FOLFOX adjuvant chemotherapy can be predicted by molecular subtype. Oncotarget 2017;8:39367-81.

Jang M, Kwon Y, Kim H, Kim H, Min BS, Park Y, et al. Microsatellite instability test using peptide nucleic acid probe-mediated melting point analysis: a comparison study. BMC Cancer 2018;18:1218.

Kim MH, Jang M, Kim H, Lee WJ, Kang CM, Choi HJ. Distinct immunological properties of the two histological subtypes of adenocarcinoma of the ampulla of Vater. Cancer Immunol Immunother 2019;68:443-54.